Current Research in Biotechnology 7 (2024) 100195

Contents lists available at ScienceDirect

Current Research in Biotechnology

journal homepage: www.elsevier.com/locate/crbiot

Lipid droplets dependent or independent cytoprotective activities of unsaturated fatty acids, Lorenzo's oil and sulfo-N-succinimidyl oleate on 7-ketocholesterol-induced oxidative stress, organelle dysfunction and cell death on 158N and ARPE-19 cells: Cell targets and benefits of sulfo-N-succinimidyl oleate

Thomas Nury [a], Imen Ghzaiel [a,b,c], Aziz Hichami [d], Claudio Caccia [e], Valerio Leoni [f], Vivien Pires [a,g], Atanas G Atanasov [h,i], Amira Zarrouk [c], Gérard Lizard [a,*], Anne Vejux [a,g,*]

[a] Team Bio-PeroxIL 'Biochemistry of the Peroxysome, Inflammation and Lipid Metabolism' (EA 7270), University Bourgogne Franche-Comté (UBFC), Inserm, Dijon, France
[b] University Clermont Auvergne, Clermont Auvergne INP, CNRS, Institut Pascal, Clermont-Ferrand 63000, France
[c] Lab-NAFS 'Nutrition-Functional Food & Vascular Health', Faculty of Medicine, University of Monastir, LR12ES05, Monastir 5000, Tunisia
[d] Physiology of Nutrition & Toxicology (NUTox), Inserm U1231, University UBFC, Dijon, France
[e] Laboratory of Medical Genetics and Neurogenetics, Fondazione IRCCS Istituto Neurologico Carlo Besta, Milan, Italy
[f] Laboratory of Clinical Pathology, Ospedale di Desio, ASST-Monza and Department of Medicine and Surgery, University of Milano-Bicocca, Italy
[g] Centre des Sciences du Goût et de l'Alimentation, CNRS, INRAE, Institut Agro, Université de Bourgogne, Dijon F-21000, France
[h] Institute of Genetics and Animal Biotechnology of the Polish Academy of Sciences, Magdalenka, Poland
[i] Ludwig Boltzmann Institute Digital Health and Patient Safety, Medical University of Vienna, Vienna, Austria

ARTICLE INFO

Keywords:
7-ketocholesterol
α-linolenic acid
Eicosapentaenoic acid
Docosahexaenoic acid
Oleic acid
Erucic acid
Lorenzo's oil
Oxiapoptophagy
Sulfo-N-succinimidyl oleate (SSO)
158N cells
ARPE-19 cells

ABSTRACT

7-ketocholesterol is a cytotoxic oxysterol which is frequently increased in many chronic inflammatory and age-related diseases. Thus, the inhibition of the toxicity of 7-ketocholesterol is a major challenge to treat these diseases. 158N oligodendrocytes were used to evaluate the cytoprotective effects of lipids: ω-3 and ω-9 fatty acids (α-linolenic acid (C18:3n-3), eicosapentaenoic acid (C20:5n-3), docosahexaenoic acid (C22:6n-3), erucic acid (C22:1n-9) and oleic acid (C18:1n-9)), Lorenzo's oil (a mixture of oleic and erucic acid, 4:1) and sulfo-N-succinimidyl oleate (SSO, a synthetic derivative of oleic acid). On 158N cells, the ability of these molecules to inhibit 7KC-induced oxiapoptophagy (plasma membrane alteration, loss of ΔΨm, peroxisomal dysfunction, reactive oxygen species overproduction, induction of apoptosis and autophagy) were determined. ARPE-19 epithelial retinal cells were also used to evaluate the cytoprotective effect of SSO on 7KC-induced cell death. Unlike ω-3 and ω-9 fatty acids and Lorenzo's oil, sulfo-N-succinimidyl oleate had no cytotoxic effects over a wide range of concentrations. Noteworthy, unlike fatty acids and Lorenzo's oil, the cytoprotective effects of sulfo-N-succinimidyl oleate on 7KC-induced oxiapoptophagy, a caspase-dependent mode of cell death on 158N cells, were not associated with an accumulation of lipid droplets. In addition, on ARPE-19 cells, sulfo-N-succinimidyl oleate prevented 7KC-induced oxidative stress and cell death. These different characteristics of SSO make it possible to envisage its use for therapeutic purposes in diseases where 7-ketocholesterol levels are increased without eventual secondary side effects due to lipid droplets formation.

Abbreviations: ALA, α-linolenic acid; AMD, age-related macular degeneration; Triol, cholestane-3β, 5α, 6β-triol; COX-2, cyclooxygenase-2; DHA, docosahexaenoic acid; DHE, dihydroethidium; $DiOC_6(3)$, 3,3′-dihexyloxacarbocyanine iodide; EA, erucic acid; DMF, dimethyl fumarate; EPA, eicosapentaenoic acid; EtOH, ethanol; FAs, fatty acids; FDA, fluorescein diacetate; GC–MS, Gas chromatography – mass spectrometry; HMOX, Heme Oxygenase; IL-6, interleukin-6; MC540, merocyanine 540; MFI, Mean Fluorescence Intensity; ΔΨm, mitochondrial membrane potential; MMF, monomethylfumarate; NPD1, neuroprotectin D1; NOS2, nitric oxide synthase 2; NRF2, Nuclear factor (erythroid-derived 2)-like 2; OA, oleic acid; ORO, Oil Red O; PMSF, phenylmethylsulfonyl fluoride; ROS, reactive oxygen species; SD, standard deviation; SOD2, Mn-superoxide dismutase 2; SR101, sulforhodamine 101; SSO, sulfo-N-succinimidyl oleate; TNF-α, tumor necrosis factor-α; VLCFAs, very long chain fatty acids; X-ALD, X-linked adrenoleukodystrophy; 7KC, 7-ketocholesterol; 24S-OHC, 24S-hydroxycholesterol; 7β-OHC, 7β-hydroxycholesterol.

* Corresponding authors at: Laboratoire Bio-PeroxIL, Université de Bourgogne, Inserm, Faculté des Sciences Gabriel, 6 boulevard Gabriel, Dijon 21000, France.
E-mail addresses: gerard.lizard@u-bourgogne.fr (G. Lizard), vejux@u-bourgogne.fr (A. Vejux).

https://doi.org/10.1016/j.crbiot.2024.100195
Received 20 February 2024; Received in revised form 27 February 2024; Accepted 4 March 2024
Available online 6 March 2024

Introduction

Cholesterol provided by the diet or formed by endogenous synthesis is one of the most abundant and physiologically important lipids in the body (Bjorkhem and Meaney, 2004). Some cholesterol oxide derivatives, called oxysterols, are downstream metabolites of cholesterol oxidation (Mutemberezi et al., 2016). They can be divided into two categories: primary and secondary oxysterols. The primary oxysterols, synthesized directly from the cholesterol, are composed of side-chain oxysterols and ring-modified oxysterols (Duc et al., 2019). The secondary oxysterols are generated from primary oxysterols. Oxysterols formed either by auto-oxidation or enzymatically, or by both processes are involved in several diseases associated with oxidative stress and rupture of RedOx homeostasis, especially age-related diseases (cardiovascular diseases, Alzheimer's disease, osteoporosis, ocular diseases (age-related macular degeneration (AMD), cataract)) but also some cancers (breast, prostate), inflammatory bowel diseases and rare diseases (Niemann-Pick's disease, Smith Lemli Opitz syndrome, X-linked adrenoleukodystrophy (X-ALD)) (Mutemberezi et al., 2016; Zarrouk et al., 2014; Nury et al., 2017; Testa et al., 2018; Samadi et al., 2021; Vigne and Pot, 2024). Among the oxysterols formed by autoxidation implying reactions catalyzed by metals, radiations or heat involving superoxide anion, hydroxyl radical, peroxide, or superoxide, the most common is 7-ketocholesterol (7KC) (Ghzaiel et al., 2022). Indeed, the 7 position on cholesterol is the most reactive with oxygen and a carbonyl group the most stable form (Anderson et al., 2020). Noteworthy, 7KC, which is also the most frequent non-enzymatically produced oxysterol (Brown and Jessup, 1999); is found at increased level in the biological fluids and tissue lesions of patients with age-related diseases, some chronic inflammatory diseases and rare diseases (Zarrouk et al., 2014; Testa et al., 2018; Brown and Jessup, 1999; Brahmi et al., 2019; Vejux et al., 2020; Mahalakshmi et al., 2021). To prevent and/or treat these diseases associated with high 7KC levels compared to healthy subjects, three strategies are currently possible. This consists either i) in promoting the degradation of 7KC (Ghosh et al., 2024); ii) in selectively removing 7KC from the cells (Bhargava et al., 2023) or iii) in acting on the signaling pathways involved in the cytotoxicity of this oxysterol (Nury et al., 2021) which induces oxidative stress and inflammation that can lead to cell death defined as oxiapoptophagy since it simultaneously triggers OXIdative stress, APOPTOsis and autoPHAGY (Nury et al., 2021; Klionsky et al., 2016; Nury et al., 2014). The alternative application of enzymes from microbial sources to degrade 7KC (medical bioremediation) *in vitro* and *in vivo* is an attractive approach developed since 2008 (Mathieu et al., 2008; Schloendorn et al., 2009). In addition to conventional pharmacological strategies, medical bioremediation is based on the use of microbial enzymes to compensate for missing catabolic functions and is a promising approach in order to overcome the insufficiency of 7KC catabolism (Schloendorn et al., 2009). UDP-003 is a novel class of cyclodextrin molecules for the encapsulation of toxic oxidized cholesterol (oxysterols) which mitigates the harmful effects of 7KC in mouse and human monocyte and macrophage cell lines (Oconnor and Clemens, 2022); interestingly, experimental evidence shows that administration of UDP-003 selectively removes 7KC from the cells and can reverse the foam cell phenotype (Bhargava et al., 2023). Pharmacological approaches consist in acting on 7KC-activated signaling pathways through strategies based on the use of: i) natural molecules (nutrients: fatty acids, polyphenols, tocopherols), oils (especially olive, argan and milk thistle seed oils) or synthetic molecules (Nury et al., 2021; Rezig et al., 2022) such as dimethylfumarate, also known as Tecfidera, employed in the treatment of chronic and inflammatory diseases as remittent-recurrent multiple sclerosis (Zarrouk et al., 2017; Bresciani et al., 2023), ii) functionalized nanoparticles (Targeted ORganelle Nano-Therapy (TORNtherapy)), or iii) chimeric molecules (Brahmi et al., 2019; Testa et al., 2014). *In vitro* and *in vivo*, several models have been used for the identification of natural and synthetic molecules as well as mixtures of compounds (oils) to prevent 7KC-induced cytotoxicity (Vejux et al., 2020). Currently, few molecules have been shown to be effective *in vitro*, in preventing 7KC-induced oxiapoptophagy (Brahmi et al., 2019; Nury et al., 2021; Yammine et al., 2020; Ghzaiel et al., 2024). These are α-tocopherol, fatty acids (FAs) (oleic acid (OA; C18:1n-9), docosahexaenoic acid (DHA; C22:6n-3)) and dimethyl fumarate, an activator of the Nrf2 pathway, as well as its major metabolite, monomethyl fumarate (Brahmi et al., 2019; Nury et al., 2021; Yammine et al., 2020). Many Mediterranean oils (argan oil, olive oil and milk thistle seed oil) have also shown cytoprotective effects against 7KC (Zarrouk et al., 2019). While the cytoprotective mechanism of α-tocopherol can be explained at least in part by its ability to prevent the accumulation of 7KC in the lipid rafts, thus opposing the activation of signals leading to cell death (Ragot et al., 2013; Royer et al., 2009), there is little information on the cytoprotection of fatty acids (FAs: OA, DHA) against 7KC (Debbabi et al., 2017; Nury et al., 2015). It can be assumed that they could both neutralize 7KC by esterification (Monier et al., 2003) and act by reducing oxidative stress and mitochondrial dysfunction leading to cell death (Brahmi et al., 2019). As OA and DHA, present in significant amounts in the Mediterranean diet (Schwingshackl et al., 2020), are often associated with dietary supplements and can be used in functional foods, it is important to have more information on these molecules, as well as on the precursors of DHA (α-linolenic acid (ALA/C18:3n-9) and eicosapentaenoic acid (EPA/C20:5n-3)), by comparing their activities, assessing their deleterious effects and specifying their mechanisms of action. In addition, it remains important to identify new molecules or mixture of molecules preventing 7KC-induced cytotoxic effects and reversing the development of associated diseases. Sulfo-N-hydroxysuccinimidyl ester of oleic acid (SSO), which has been described to bind and inhibit CD36 (Coort et al., 2002), is an analogue of OA: evaluating the cytoprotective effects of SSO comparatively to OA on 7KC-treated cells is consequently of interest. On neurons and BV-2 co-cultures, as well as on neurons and primary microglia co-cultures, SSO also significantly reduced the lipopolysaccharide/interferon-γ-induced production of nitric oxide, interleukin-6 (IL-6), tumor necrosis factor-α (TNF-α), and the protein levels of inflammatory enzymes including nitric oxide synthase 2 (NOS2), cyclooxygenase-2 (COX-2), and p38 mitogen-activated protein kinase in microglia, without causing cell toxicity (Dhungana et al., 2017). On isolated rat liver mitochondria, SSO modulates mitochondrial membrane potential (ΔΨm) and mitochondrial complex III activity (Drahota et al., 2010). Independently of its activities on CD36, SSO could therefore act on other cellular targets. Furthermore, as X-ALD is associated with elevated plasma levels of 7KC (Nury et al., 2017), and since Lorenzo's oil (composed of oleic acid (C18:1n-9) and erucic acid (C22:1n-9) in a ratio of 4:1) is sometimes administered to patients with X-ALD in an attempt to prevent neurodegeneration by reducing levels of very long-chain fatty acids (VLCFAs), oxidative stress and inflammation as well as demyelination (Prieto Tenreiro et al., 2013), it was also considered as essential to determine the effect of Lorenzo's oil on 7KC-induced cytotoxicity.

In the present study, we evaluated and compared the cytoprotective effects of unsaturated fatty acids (ALA, EPA, DHA, OA, EA) and SSO as well as of Lorenzo's oil (OA and EA in a ratio of 4:1) on 7KC-treated 158N cells which is a relevant model to identify natural or synthetic molecules able to prevent 7KC-induced cytotoxicity and to determine the relationship between oxidative stress, apoptosis and autophagy as well as the part played by organelles (mitochondria, peroxisomes) in these processes (Vejux et al., 2020). We also evaluated the cytoprotective effects of OA and its synthetic analog SSO on ARPE-19 human epithelial retinal cell line since important 7KC deposits are present in drusens which are abnormal deposits localized under the retina between the Bruch's membrane and the retinal pigment epithelium of the eye in patients with age-related macular degeneration (AMD) (Rodríguez and Larrayoz, 2010; Pariente et al., 2019; Zhang and Sivaprasad, 2021). The effects of these compounds, SSO and Lorenzo's oil, were compared with those of α-tocopherol, the major component of Vitamin E, composed of a mixture of four tocopherols and four tocotrienols (Rimbach et al., 2002),

and which was used as reference cytoprotective molecule. Although all compounds tested, excepted EA, attenuated the toxicity of 7KC, SSO had the most interesting and promising profile for potential therapeutic applications: our data show that it was not cytotoxic even at high concentrations and did not induced cytoplasmic accumulation of lipid droplets. In addition, the ability of SSO to attenuate 7KC-induced reactive oxygen species (ROS) overproduction and plasma membrane alteration was accompanied by a restoration of cell signaling that controls ΔΨm and prevents cell death.

Methods

Cell culture and treatments

Murine oligodendrocytes (158N) (Baarine et al., 2009) and human ARPE-19 epithelial retinal cells (Dugas et al., 2010) were seeded at 30,000 cells/cm2 either in 100 mm diameter Petri dishes, 12 wells plates or 96 wells plates. They were cultured in Dulbecco's Modified Eagle Medium (DMEM) (Lonza, Lonza, Amboise, France) containing 5 % (for 158N) or 10 % (for ARPE-19) (v/v) heat-inactivated fetal bovine serum (Dutscher, Brumath, France) and 1 % antibiotics (penicillin, streptomycin) (Pan Biotech Aidenbach, Germany). The incubation was performed at 37 °C in a humidified atmosphere containing 5 % CO_2. For subcultures, cells were trypsinized (0.05 % trypsin-0.02 % EDTA solution) and passaged twice a week. 7-ketocholesterol (7KC; Sigma-Aldrich/Merck, St Quentin-Fallavier, France, ref C2394) stock solution was prepared at 2 mM as previously described (Ragot et al., 2013). After 24 h of culture, 158N cells were incubated for 24 h with 7KC, α-tocopherol (Sigma-Aldrich/Merck, ref T3251), α-linolenic acid (ALA; Sigma-Aldrich/Merck, ref L2376), eicosapentaenoic acid (EPA; Enzo Life Sciences, ref BML-FA001-0100), docosahexahenoic acid (DHA; Sigma-Aldrich/Merck, ref D2534), oleic acid (OA; Sigma-Aldrich/Merck, ref 01008), erucic acid (EA; Interchim, Montluçon, France: ref DRE-C13203000), Lorenzo's oil (OA + EA: ratio 4:1) or sulfo-N-succinimidyl oleate (SSO; Interchim, ref 11211), or with 7KC associated with α-tocopherol, ALA, EPA, DHA, OA, EA, Lorenzo's oil or SSO. FAs stock solutions were prepared at 50 mM (ALA, DHA, OA, EA) or 200 mM (EPA) in absolute ethanol (Carlo-Erba, Val de Reuil, France) and stored at −20 °C. SSO stock solution was prepared at 50 mM in dimethylsulfoxide (DMSO, Sigma-Aldrich/Merck). The activator of autophagy (Rapamycin (Sigma-Aldrich/Merck; ref 37094)), the inhibitor of autophagy (3-methyl adenine (Sigma-Aldrich/Merck; ref M9281)) and the inhibitor of apoptosis (z-VAD-fmk, Bachem, Bubendorf, Switzerland; ref 4026865) were prepared and used as previously described (Doria et al., 2019; Sassi et al., 2019; Vejux et al., 2007).

Measurement of cell viability with the fluorescein diacetate (FDA) assay

The cell-permeant esterase substrate fluorescein diacetate (FDA) assay (Invitrogen/Thermofisher Scientific, ref F1303) was used as a viability probe (Namsi et al., 2018). At the end of the treatment, cells were incubated in the dark with FDA (15 μg/mL in PBS, 5 min, 37 °C) and rinsed with PBS. Cell fluorescence intensity (Ex: 485 nm/Em: 538 nm) was measured with a TECAN fluorescence microplate reader (Sunrise spectrophotometer, TECAN, Lyon, France). The experiments were realized in triplicate. The data were expressed as percentage of control.

Quantification of adherent cells with the sulforhodamine 101 (SR101) assay

Suforhodamine 101 (SR101; Sigma-Aldrich/Merck, ref S7635) assay was used to evaluate the number of adherent cells by its ability to stain the total cellular protein content (Namsi et al., 2019). At the end of treatments, cells were fixed with ethanol 70 % for 20 min at 4 °C. After two washes in PBS, cells were stained with a SR101 solution (1.5 μg/mL, 30 min, 4 °C). Then, the cells were washed twice with PBS and the fluorescence was measured with a fluorescent plate reader (Infinite M200, TECAN) using Ex 535 nm/Em 610 nm. The experiments were realized three times in triplicate, and the data were expressed as percentage of control.

Cell condition assessment with morphological criteria by phase contrast microscopy

Cells were seeded in 12 well plates and treated with or without 7KC, FAs, Lorenzo's oil, SSO and α-tocopherol for 24 h. At the end of the treatments, cells were observed under an inverted phase contrast microscope (Primovert Zeiss microscope, Jena, Germany) at a x20 magnification. Digitalized images were obtained with a Zeiss camera (5MP HD IP).

Flow cytometric quantification of mitochondrial transmembrane potential (ΔΨm) with $DiOC_6(3)$

Modifications of ΔΨm were measured with 3,3′-dihexyloxacarbocyanine iodide ($DiOC_6(3)$) (ThermoFischer Scientific, Courtaboeuf, France). At the end of treatments, cells were trypsinized and resuspended in PBS containing $DiOC_6(3)$ used at 40 nM. Cells were incubated for 15 min at 37 °C in the dark. Cells were analyzed with a BD Accuri C6 flow cytomer (Becton-Dickinson, La Jolla, CA, USA); the green fluorescence was collected through a 520/10 nm band pass filter and analyzed on a logarithmic scale: 10,000 cells were acquired. The percentage of $DiOC_6(3)$ negative cells was determined using the FlowJo software (Tree Star Inc, Ashland, OR, USA).

Flow cytometric measurement of the loss of asymmetry and altered packing of the plasma membrane with merocyanine 540

Merocyanine 540 (MC540) (Sigma-Aldrich/Merck) is a negatively charged chromophore that binds to the outer leaflet of the cell membrane; the loss of asymmetry and altered packing of the membrane enhance MC540 fluorescence (Schlegel et al., 1993; Vejux et al., 2009). MC540 was prepared in absolute ethanol at 2.5 mg/mL. At the end of treatments, adherent and non-adherent cells were collected and resuspended in culture medium containing MC540 (2.5 μg/mL). Cells were incubated (10 min, room temperature (RT)), and analyzed with a BD Accuri C6 flow cytometer (Becton-Dickinson). The orange/red fluorescence was collected through a 590/20 nm band pass filter and analyzed on a logarithmic scale: 10,000 cells were acquired. The percentage of MC540 positive cells was determined using the FlowJo software (Tree Star Inc).

Flow cytometric quantification of reactive oxygen species after staining with dihydroethidium

The overproduction of reactive oxygen species (ROS) was detected with dihydroethidium (DHE; Life Technologies, St. Aubin, France) (Rothe and Valet, 1990; Baarine et al., 2012). DHE was prepared at 1.6 mM in DMSO and used at 2 μM in PBS. Cells were incubated (15 min, RT), and analyzed with a BD Accuri C6 flow cytometer (Becton-Dickinson); the orange/red fluorescence was collected through a 590/20 nm band pass filter and analyzed on a logarithmic scale: 10,000 cells were acquired. The percentage of DHE positive cells were determined using FlowJo software (Tree Star Inc).

Visualization of lipid droplets with oil red O (ORO): Observation with brightfield microscopy

Lipid droplets are dynamic organelles and function as a storage depot for neutral lipids, including triglycerides and cholesterol esters (Walther and Farese, 2012). The presence of neutral lipids was investigated by

staining with Oil Red O (ORO; Sigma-Aldrich/Merck). ORO is soluble in neutral lipids and remains dissolved in triglycerides after washing. Thus, at the end of treatments, 158N cells cultured in 6 well-plates were washed with PBS and stained with ORO solution (three parts 0.5 % ORO dye in isopropanol into two parts water) for 30 min and stored in the dark at RT (Debbabi et al., 2017). The stained cells were washed three times with water and three contiguous observation fields always taken in the center of a 6-well plate were observed under an inverted phase contrast microscope (Axiovert 40 CFL, Zeiss).

Visualization by fluorescence microscopy and quantification by flow cytometry of lipid droplets stained with Bodipy 493/503

The presence of lipid droplets was also analyzed with the fluorescent neutral lipid dye 4,4-difluoro-1,3,5,7,8-pentamethyl-4-bora-3a,4a-diaza-s-indacene (Bodipy 493/503) (Sigma-Aldrich/Merck, ref 790389) which permits the observation of the lipid droplets by fluorescence microscopy and their quantification by flow cytometry (Qiu and Simon, 2016). For microscopical analysis, cells were seeded on glass slides in 12 well plates. After 24 h of culture, cells were incubated with 7KC for 24 h without or with α-tocopherol, FAs, Lorenzo's oil or SSO. After treatments, cells were washed with PBS and stained with Bodipy 493/503 (2 μM; 15 min; 37 °C). After washing, cells were fixed with 4 % paraformaldehyde (10 min at RT, in the dark) and washed again with PBS. A counterstaining with Hoechst 33342 (2 μg/mL in PBS, 5 min at RT, in the dark) was realized. The slides were mounted in fluorescent mounting medium (Dako), stored in the dark at 4 °C, and examined under a right fluorescence microscope (Axioskop, Zeiss). For flow cytometry, cells were trypsinized and stained in the same conditions (no counterstaining with Hoechst 33342 was realized). Cell suspensions were analyzed with a BD Accuri C6 flow cytometer (Becton-Dickinson); the green fluorescence was collected through a 520/10 nm band pass filter and analyzed on a logarithmic scale: 10,000 cells were acquired. The mean fluorescence intensities of Bodipy 493/503 samples were determined using FlowJo software (Tree Star Inc).

Quantification of 7-ketocholesterol and fatty acids, including very long chain fatty acids, by gas chromatography coupled with mass spectrometry

7KC and FAs were quantified on untreated and treated 158N cells as previously described (Leoni et al., 2017). Cellular homogenates, prepared from pellets of about 10^7 cells suspended in water (100 μL) and sonicated for 10 min, were added to a screw capped vial sealed with a Teflon septum together with structural homologous internal standards (pentadecanoic 50 μg, heptadecanoic acid 100 μg, nonadecanoic acid 5 μg, heneicosanoic acid, 2.5 μg, tricosanoic acid 1 μg, epicoprostanol 50 μg), butylated hydroxytoluene and EDTA, and flushed with argon for 10 min to remove air. Alkaline hydrolysis was allowed to proceed at room temperature (22 °C) with magnetic stirring for 60 min in the presence of ethanolic 0.5 M potassium hydroxide solution. Sterols and oxysterols were collected by liquid to liquid extraction with 5 mL of hexane. FAs were collected after correction of pH (<3) with HCl by liquid to liquid extraction with hexane and ethylacetate. The organic solvents were evaporated under a gentle stream of argon and converted into trimethylsilyl ethers with bis(trimethylsilyl)trifluoroacetamide with 1 % trimethylchlorosilane (Pierce/ThermoFisher Scientific).

Gas chromatography – mass spectrometry (GC–MS) analysis was performed on an Agilent 5973 Mass spectrometer connected to a GC 6890 Agilent equipped with an HP-5MS columns (30 m × 0.32 mm internal diameter (id) × 0.25 mm film; Agilent, USA) and injection was performed in splitless mode using helium (1 mL/min) as carrier gas. The temperature program was as follows: initial temperature 150 °C was held for 1 min, followed by a linear ramp of 10 °C/min to 250 °C, 20 °C/min to 300 °C and held for 5 min. The mass spectrometer operates in full mass scan mode. Peak integration was performed manually, and metabolites were recognized by retention time and fragmentation patterns and quantified from total-ion count against internal standards using standard curves for the measured FAs, cholesterol and 7KC. Recovery ranged between 94 % up to 100 % and precision ranged between 3 up to 7 %.

Quantification of gene expression by RT-qPCR

Total mRNA from 158N cells were extracted and purified using the RNeasy Mini Kit (Qiagen, Courtaboeuf, France) and the total mRNA concentration was measured with TrayCell (Hellma, Paris, France). The purity of nucleic acids was controlled by the ratio of absorbance at 260 nm and 280 nm (ratios between 1.8–2.2). 1 μg of mRNA was used for reverse transcription using the iScript cDNA Synthesis Kit (Bio-Rad, Marne La Coquette, France) according to the following protocol: 5 min at 25 °C, 20 min at 46 °C, 5 min at 95 °C. cDNA were generated using the FG Power SYBR Green (ThermoFischer Scientific). PCR reactions were realized on an Applied Biosystem Step One plus QPCR machine (Life Science Technologies/ThermoFisher Scientific). The primer sequences were the following:

- **HMOX:** forward 5′- cacagcactatgtaaagcgtct −3′ reverse 5′- gtagcgggtatatgcgtggg −3′
- **SOD2:** forward 5′- ggaagccatcaaacgtgact −3′ reverse 5′- ctgatttggacaagcagcaa −3′
- **Catalase**: forward 5′-agcgaccagatgaagcagtg-3′ reverse 5′-tccgctctctgtcaaagtgtg-3′
- ***36B4****: forward 5′-gcgacctggaagtccaacta −3′ reverse 5′-atctgcttggagcccacat −3′*

Thermal cycling conditions were as follows: activation of DNA polymerase at 95 °C for 10 min, followed by 40 cycles of amplification at 95 °C for 15 s, 60 °C for 30 s, and 72 °C for 30 s, followed by a melting curve analysis to test for the absence of non-specific products. Gene expression was quantified using cycle threshold (Ct) values and normalized by the 36B4 reference gene. The quantitative expression of catalase was determined as fold induction of the control.

Protein analysis by SDS-page and Western blotting

Protein analysis was realized as previously described by polyacrylamide gel electrophoresis and Western blotting (Nury et al., 2015; Nury et al., 2018; Ragot et al., 2011). Cells washed in PBS were lysed in a RIPA buffer (10 mM Tris-HCl, pH 7.2, 150 mM NaCl, 0.5 % Nonidet NP40, 0.5 % Na deoxycholate, 0.1 % SDS, 2 mM EDTA and 50 mM NaF) in the presence of 1/25 complete protease inhibitor cocktail tablets (Roche Diagnostics, Indianapolis, IN, USA) and phenylmethylsulfonyl fluoride (PMSF; Sigma-Aldrich/Merck, 1 mM) for 30 min on ice. Cell lysates were cleared by a 20 min centrifugation at 12,000 g. The protein concentration in the supernatant was measured using the Bicinchoninic Acid Assay kit (Sigma-Aldrich/Merck). Seventy micrograms of protein were diluted in loading buffer (125 mM Tris- HCl, pH 6.8, 10 % β-mercaptoethanol, 4.6 % SDS, 20 % glycerol, and 0.003 % bromophenol blue), separated on a 8 % or 14 % SDS-PAGE gel depending of the molecular weight of the proteins, and transferred onto a nitrocellulose membrane (Bio-Rad, Marne La Coquette, France). After blocking nonspecific binding sites for 1 h with 5 % milk powder in PBST (PBS, 0.1 % Tween 20, pH 7.2), the membrane was incubated overnight at 4 °C with the primary antibody diluted in PBST + 5 % milk powder. The antibodies raised against caspase-3 (rabbit polyclonal antibody; Ozyme/Cell Signaling/Clinisciences, Nanterre, France; ref: 9662; detecting endogenous levels of full length casapase-3 (35 kDa) and the large fragment of caspase-3 resulting from cleavage (17 kDa)), and LC3 (rabbit polyclonal antibody; Sigma-Aldrich/Merck, ref L8918; detecting LC3-I (18 kDa) and LC3-II (16 kDa)), Mcl-1 (monoclonal antibody; Abcam, Cambridge, UK: ref ab32087), Phospho-Mcl-1 (Ser159/Thr163) (rabbit polyclonal antibody; Ozyme/Cell Signaling/Clinisciences; ref

4579), Bad (rabbit polyclonal antibody; Ozyme/Cell Signaling/Clinisciences; ref 9292), PARP (rabbit monoclonal antibody; Ozyme/Cell Signaling/Clinisciences; ref 9532; detecting endogenous levels of full length PARP (110 kDa) and the fragment of PARP resulting from cleavage (89 kDa)), NRF2 (rabbit polyclonal antibody; Tebu-Bio, Le Perray-en-Yvelines, France: ref 0279–2), Phospho-NRF2 (ser40) (Rabbit Monoclonal Antibody; ThermoFischer Scientific: ref 16335544) were used at 1/1,000 final dilution. The antibody directed against β-actin (mouse monoclonal antibody; Sigma-Aldrich/Merck, ref A2228) was used at a final concentration of 1/10,000. The membrane was then washed with PBST and incubated for 1 h at RT with horseradish peroxidase-conjugated goat anti-rabbit (Cell Signaling/Clinisciences, ref 7074) or anti-mouse antibody (Santa-Cruz Biotechnology, Santa Cruz, CA, USA: ref sc-2005) diluted at 1/5,000. The membrane was washed with PBST and revealed using an enhanced chemiluminescence detection kit (Supersignal West Femto Maximum Sensitivity Substrate, ThermoFisher Scientific) and Chemidoc XRS+ (Bio-Rad). The level of bands intensity was measured with Image Lab software (Bio-Rad).

Wound healing/cell migration assay

ARPE-19 cells were seeded in 12 well plates to obtain a confluent cell monolayer after 24 h of culture. Cell monolayers were scratched with a p1000 pipette tip to induce a wound, and images were taken on an inverted phase contrast microscope (Primovert Zeiss microscope) at x10 magnification. Digitalized images were obtained with a Zeiss camera (5MP HD IP) to measure the wound size. Cells were then treated with 7KC (100 μM) with or without OA (100 μM), SSO (50 μM), and α-tocopherol (400 μM). 24 h later, a new image was taken, and the wound size was also measured. The cell migration was evaluated by the distance of cell migration in each condition. The experiments were realized three times in triplicate, and the data were expressed as fold induction comparing to untreated cells.

Statistical analysis

The experimental data represent the mean ± standard deviation (SD). Statistical analyses were performed using XLStat software. The Mann-Whitney *U* test was used to compare the different groups, and data were considered statistically different at a *P* value of 0.05 or less.

Results

Comparative study of the effects of α-linolenic acid (ALA), eicosapentaenoic acid (EPA), docosahexaenoic acid (DHA), oleic acid (OA), erucic acid (EA), Lorenzo's oil (OA + EA; 4:1) and sulfo-N-succinimidyl oleate (SSO) on cell growth and viability of 158N oligodendrocytes.

On 158N cells, FAs (ALA, EPA, DHA, OA, EA) and SSO were used alone in a concentration range from 25 to 200 μM for a 24 h treatment. Lorenzo's oil was used at different concentrations of EA and OA (OA not exceeding 200 μM). α-tocopherol was used from 100 to 400 μM (Ragot et al., 2013). With the FDA and SR101 assays, no cytotoxic effect of α-tocopherol was observed and with SSO, a slight decrease on cell growth was found at 200 μM with the SR101 assay (Fig. 1). More or less marked cytotoxic effects were observed with FAs and Lorenzo's oil. Thus, as early as 100 μM, ALA, EPA and DHA showed cytotoxic effects with FDA and SR101 assays (Fig. 1). OA shows pronounced toxicity only at 200 μM with the FDA assay (Fig. 1). EA only shows slight cytotoxic effects at 200 μM (Fig. 1). With Lorenzo's oil, pronounced effects on the inhibition of cell growth measured by the SR101 assay were detected as early as the [AO (100 μM)/EA (25 μM)] concentrations (Fig. 1). To subsequently evaluate the eventual cytoprotective effects of these FAs on 7KC-induced oxidative stress, mitochondrial and peroxisomal dysfunctions and cell death (apoptosis, autophagy), the highest non cytotoxic concentrations were selected: ALA (50 μM); EPA (50 μM); DHA (50 μM); OA (100 μM); EA (25 μM); SSO (50 μM). Consequently, the Lorenzo's oil ratio chosen was (OA: 100 μM/EA: 25 μM; ratio 4:1).

Evaluation with the FDA and SR101 assays of the cytoprotective effects of α-linolenic acid, eicosapentaenoic acid, docosahexaenoic acid, oleic acid, erucic acid, Lorenzo's oil and sulfo-N-succinimidyl oleate (SSO) on 7-ketocholesterol-treated 158N and ARPE-19 cells.

On 158N oligodendrocytes, the effects of ALA (50 μM), EPA (50 μM), DHA (50 μM), OA (100 μM), EA (25 μM), SSO (50 μM) and Lorenzo's oil (OA: 100 μM/EA: 25 μM) as well as α-tocopherol (400 μM) associated or not with 7KC (50 μM) were evaluated with the FDA and SR101 assays after 24 h of treatment (Fig. 2A and B). The concentrations of 7KC used on 158N cells was 50 μM; this concentration was chosen because it inhibits cell viability (FDA assay) and cell growth (SR101 assay) in a range of 30–50 % which was confirmed by observations realized by phase contrast microscopy (Fig. 2; Supplementary Fig. 1). On 158N cells, no cytoprotection was found with EA; however, cytoprotective effects in the same range or higher than those observed with α-tocopherol were detected with ALA, EPA, DHA, OA, SSO and Lorenzo's oil (Fig. 2A and B; supplementary Fig. 1). The results obtained with the FDA and SR101 assays were in agreement with the observations realized by phase contrast microscopy: the cytotoxic effects of 7KC characterized by a decrease in the number of adherent cells and by an increase in the number of dead cells (round cells floating in the culture medium) were strongly attenuated by ALA, EPA, DHA, OA, SSO, Lorenzo's oil and α-tocopherol whereas no cytoprotection was observed with EA (**Supplementary Fig. 1**).

On ARPE-19 retinal epithelial cells, the effects of OA (100 μM), SSO (50 μM) and the combination (OA + α-tocopherol) were evaluated with the FDA and SR101 assays after 24 h (Fig. 2C and D). The concentrations of 7KC used on ARPE-19 cells was 100 μM; this concentration was chosen because it inhibits cell viability (FDA assay) and cell growth (SR101 assay) in a range of 30–50 % (Fig. 2). On ARPE-19 cells, significant cytoprotective effects were observed both with OA, SSO, α-tocopherol and (α-tocopherol + SSO). The combination (α-tocopherol + SSO) was higher than SSO but similar than α-tocopherol alone (Fig. 2). In addition, the ability of 7KC-induced cell death to impair the capacity of the cells to recolonize a lesion was evaluated on ARPE-19. To this end, a wound healing/recolonization assay was realized on ARPE-19 cells treated with OA (100 μM), SSO (50 μM) and α-tocopherol (400 μM) associated or not with 7KC (100 μM). The data obtained showed that 7KC strongly impair the recolonization capacity of ARPE-19 cells (Fig. 3). This cytotoxic effect of 7KC was reduced by OA, SSO, α-tocopherol and (α-tocopherol + SSO), this later being the most effective (Fig. 3).

Cytoprotective effects of SSO were thus observed both on 158N and ARPE-19 cells. These data show that the cytoprotection with SSO does not depend on neither of the cell specie (murine, human) nor of the cell type (nervous, epithelial) considered. This led us to determine whether, the cytoprotection with SSO was also efficient on other cytotoxic oxysterols. On 158N cells, the cytoprotective effects obtained with SSO (50 μM) as well as OA (100 μM) were not limited to 7KC. Indeed, SSO and OA attenuated cell death induced by 24S-hydroxycholesterol (24S-OHC; 30 μM) and cholestane-3β, 5α, 6β-triol (Triol; 12.5 μM). However, SSO and OA did not protect against 7β-hydroxycholesterol (7β-OHC; 30 μM)-induced cell death (Supplementary Fig. 2).

Prevention of 7-ketocholesterol-induced mitochondrial and peroxisomal dysfunction by α-linolenic acid, eicosapentaenoic acid, docosahexaenoic acid, oleic acid, Lorenzo's oil and sulfo-N-succinimidyl oleate on 158N and ARPE-19 cells.

In the presence of 7KC (50 μM on 158N cells; 100 μM on ARPE-19 cells) after 24 h of treatment, a drop of mitochondrial transmembrane potential (ΔΨm) was revealed with $DiOC_6(3)$ (Fig. 4A and B). On 158N cells, the drop of ΔΨm (characterized by an increased percentage of cells with depolarized mitochondria; $DiOC_6(3)$ negative cells) was counteracted by ALA, EPA, DHA, OA, Lorenzo's oil and SSO but not by EA (Fig. 4A). On ARPE-19 cells, the drop of ΔΨm induced by 7KC was also

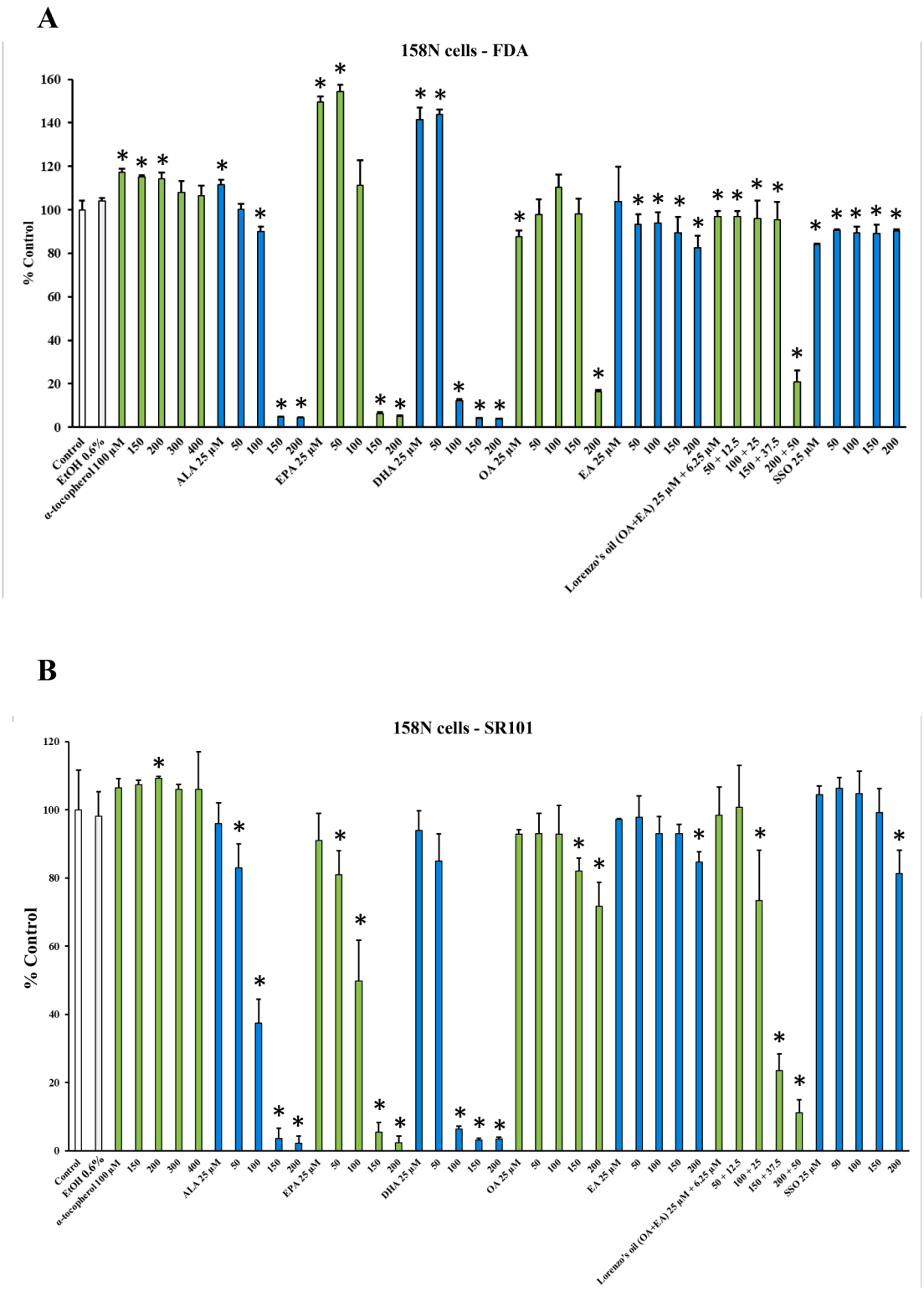

Fig. 1. Evaluation of the cytotoxicity α-linolenic acid, eicosapentaenoic acid, docosahexaenoic acid, oleic acid, erucic acid, Lorenzo's oil and sulfo-N-succinimidyl oleate with the fluorescein diacetate and sulforhodamine 101 assays. 158N cells previously cultured for 24 h were further incubated with FAs (α-linolenic acid (ALA), eicosapentaenoic acid (EPA), docosahexaenoic acid (DHA), oleic acid (OA), erucic acid (EA)), sulfo-N-succinimidyl oleate (SSO), and Lorenzo's oils (OA + EA; 4:1) as well as α-tocopherol (reference cytoprotective molecule) used alone for a 24 h additional period. At the end of the treatment, the cytotoxicity was evaluated with the FDA and SR101 assays. Data are expressed as mean ± standard deviation (SD) of three independent experiments performed in triplicate. Significance of the differences between control (untreated cells) and EtOH (0.6 %), ALA, EPA, DHA, OA, EA, SSO and Lorenzo's oil-treated cells; Mann Whitney test: * $P \leq 0.05$. No significant differences were observed between control (untreated cells) and vehicle control (Ethanol (EtOH) 0.6 %).

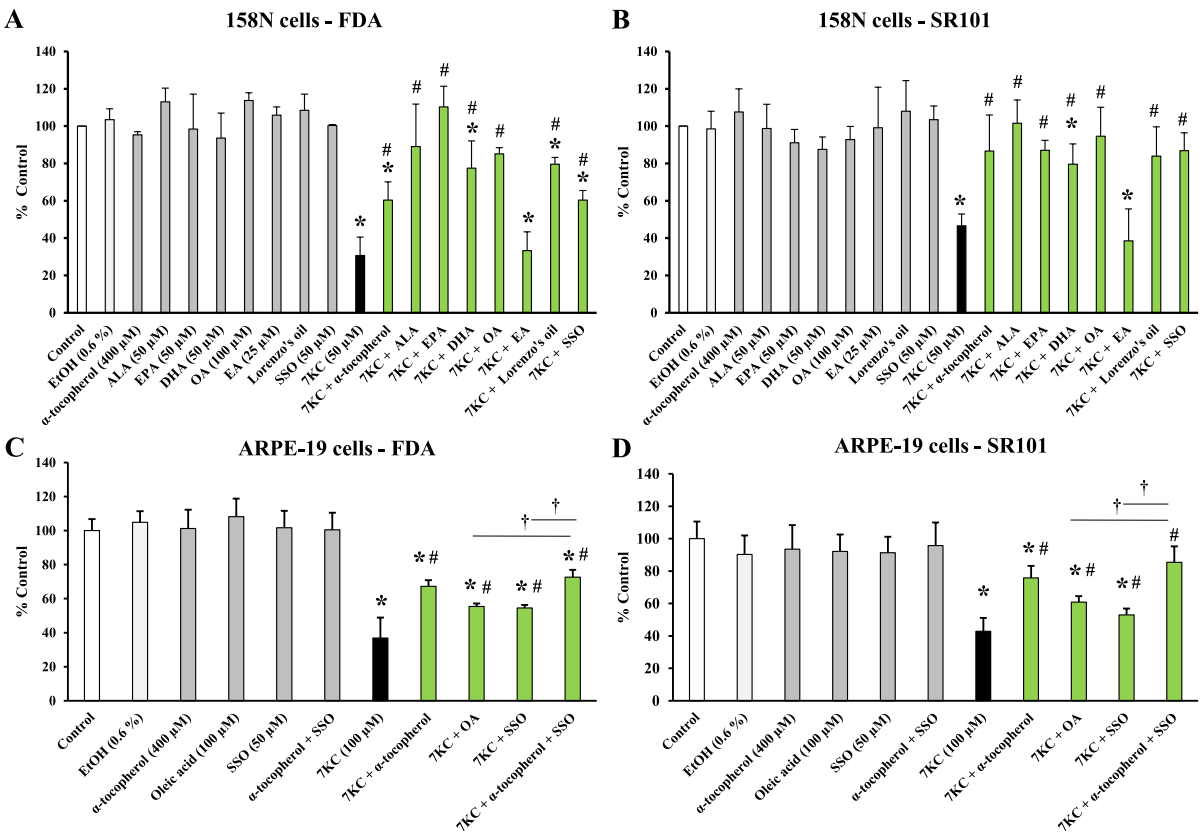

Fig. 2. Evaluation with the fluorescein diacetate and sulforhodamine 101 assays on 158N and ARPE-19 cells of the cytoprotective effects of α-linolenic acid, eicosapentaenoic acid, docosahexaenoic acid, oleic acid, erucic acid, sulfo-N-succinimidyl oleate and Lorenzo's oil on 7-ketocholesterol induced-cytotoxicity. 158N and ARPE-19 cells previously cultured for 24 h were further incubated for a 24 h additional period with 7-ketocholesterol, FAs (α-linolenic acid (ALA), eicosapentaenoic acid (EPA), docosahexaenoic acid (DHA), oleic acid (OA), erucic acid (EA)), sulfo-N-succinimidyl oleate (SSO), or Lorenzo's oils (OA + EA; 4:1) as well as α-tocopherol (reference cytoprotective molecule) and with 7KC associated with ALA, EPA, DHA, OA, EA, SSO, Lorenzo's oil or α-tocopherol. At the end of the treatment, the cytotoxicity of 7KC and the cytoprotective effects of ALA, EPA, DHA, OA, EA, SSO, Lorenzo's oil and α-tocopherol were evaluated with the fluorescein diacetate (FDA) and sulforhodamine 101 (SR101) assays. Data are expressed as mean ± standard deviation (SD) of three independent experiments performed in triplicate. Significance of the differences between control (untreated cells) and EtOH (0.6 %), ALA, EPA, DHA, OA, EA, SSO, Lorenzo's oil, α-tocopherol, 7KC, and (7KC + (ALA, EPA, DHA, OA, EA, SSO, Lorenzo's oil, or α-tocopherol))-treated cells; Mann Whitney test: * $P \leq 0.05$. Significance of the differences between 7KC-treated cells and (7KC + (ALA, EPA, DHA, OA, EA, SSO, Lorenzo's oil or α-tocopherol)-treated cells; Mann Whitney test: # $P \leq 0.05$; Significance of the differences between (7KC + (α-tocopherol + SSO)) and (7KC + α-tocopherol) or (7KC + SSO) † $P \leq 0.05$. No significant differences were observed between control (untreated cells) and vehicle control (Ethanol (EtOH) 0.6 %).

attenuated in the presence of OA, SSO, α-tocopherol and (α-tocopherol + SSO) (Fig. 4B). The combination (α-tocopherol + SSO) has a slight better efficiency than SSO and α-tocopherol used alone; the combination (α-tocopherol + SSO) was more efficient than SSO and α-tocopherol alone (Fig. 4B).

Peroxisomal dysfunctions were also evaluated on 158N cells (Fig. 4C). As very long chain fatty acids (VLCFAs: C24:0, C24:1, C26:0 and C26:1) are degraded in the peroxisome by β-oxidation (Wanders and Waterham, 2006), the intracellular levels of VLCFAs were measured: an intracellular accumulation of VLCFAs (C24:0, C24:1, C26:0 and C26:1) was observed (Fig. 4C). When ALA, EPA, DHA, OA, SSO, Lorenzo's oil and α-tocopherol were associated with 7KC, they strongly reduced the increase in VLCFAs (Fig. 4C). This supports that these compounds attenuate peroxisomal dysfunctions and re-establish peroxisomal β-oxidation. No benefit was observed with EA (Fig. 4C).

Evaluation of the effects of α-linolenic acid, eicosapentaenoic acid, docosahexaenoic acid, oleic acid, erucic acid, Lorenzo's oil and sulpho-N-succinimidyl oleate on 7-ketocholesterol-induced plasma membrane lipid disorganization.

On 158N cells, the cytoprotective effects of unsaturated fatty acids (ALA (50 µM), EPA (50 µM), DHA (50 µM), OA (100 µM), EA (25 µM), SSO (50 µM)), Lorenzo's oil (OA: 100 µM/EA: 25 µM) and SSO (50 µM) as well as α-tocopherol (400 µM), used as positive cytoprotective control, were evaluated on 7KC-treated cells after staining with MC540 which provides information on lipid membrane organization (Vejux et al., 2009) (Fig. 5 A). In addition, cholesterol, which is also a major component of plasma membrane, was quantified (Cooper, 1978) (Fig. 5B). Comparatively to untreated cells and vehicle (EtOH (0.6 %))-treated cells, no effect on plasma membrane organization measured with MC540 and cholesterol content was detected with ALA, EPA, DHA, OA, EA, SSO, Lorenzo's oil and α-tocopherol (Fig. 5A and B). However, in the presence of 7KC, the lipid organization of the plasma membrane was strongly disturbed: the percentage of MC540 positive cells (cells strongly stained by MC540) was increased (Fig. 5A) and the total cholesterol level per cell was decreased (Fig. 5B). The plasma membrane lipid disorders induced by 7KC were strongly attenuated with ALA, EPA, DHA, OA, SSO and Lorenzo's oil as well as with α-tocopherol whereas EA was inefficient (Fig. 5A). The decrease of cholesterol level induced by 7KC was normalized with EPA and OA and was not significantly attenuated by ALA, DHA, EA and Lorenzo's oil. No benefit of SSO was found (Fig. 5B).

Prevention of 7-ketocholesterol-induced oxidative stress by α-linolenic acid, eicosapentaenoic acid, docosahexaenoic acid, oleic acid, Lorenzo's oil and sulfo-N-succinimidyl oleate.

7KC-induced ROS overproduction was previously reported on 158N and ARPE-19 cells (Dugas et al., 2010; Nury et al., 2018). It was

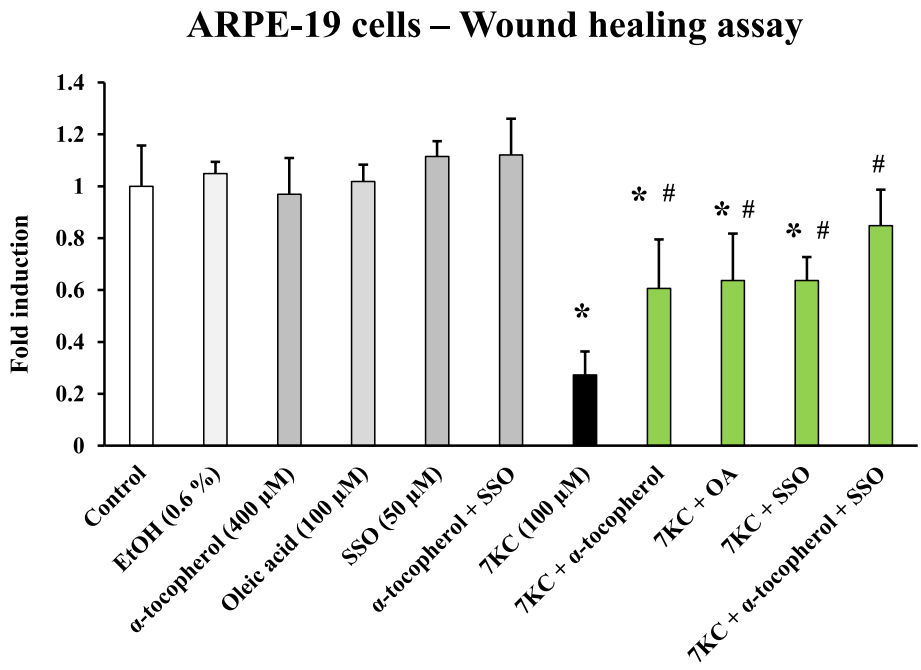

Fig. 3. Stimulation of wound healing by sulfo-N-succinimidyl oleate and oleic acid. The ability of sulfo-N-succinimidyl oleate (SSO), oleic acid (OA), α-tocopherol and (α-tocopherol + SSO) to favor wound healing was determined on 7KC-treated ARPE-19 cells. ARPE-19 cell monolayer was scratched with a p1000 pipette tip to induce a wound, and the cells were further incubated for a 24 h period with 7-ketocholesterol (7KC; 50 μM) with or without SSO (50 μM), OA (100 μM), α-tocopherol (400 μM) (used as positive cytoprotective reference) and (α-tocopherol + SSO). Significance of the differences between control (untreated cells), EtOH (0.6 %), α-tocopherol, OA, SSO, 7KC, or (7KC + α-tocopherol, OA, SSO, or (α-tocopherol + SSO)); Mann Whitney test: * $P \leq 0.05$. Significance of the differences between 7KC-treated cells and (7KC + (α-tocopherol, OA, SSO, or (α-tocopherol + SSO))-treated cells; Mann Whitney test: # $P \leq 0.05$; No significant differences were observed between control (untreated cells) and vehicle control (Ethanol (EtOH) 0.6 %).

therefore of interest to precise the effects of unsaturated fatty acids (ALA (50 μM), EPA (50 μM), DHA (50 μM), OA (100 μM), EA (25 μM)), SSO (50 μM) and Lorenzo's oil (EA: 25 μM/OA: 100 μM) as well as α-tocopherol (400 μM), used as positive control, on 7KC-induced oxidative stress (Fig. 6). On 7KC-treated 158N and ARPE-19 cells, a strong increase of the percentage of cells overproducing ROS (% DHE positive cells) was observed (Fig. 6A and B). ROS overproduction was strongly reduced by ALA, EPA, DHA, OA, Lorenzo's oil and SSO but not by EA on 158N cells (Fig. 6A). On ARPE-19 cells, ROS overproduction was also strongly reduced by OA, SSO, α-tocopherol and (α-tocopherol + SSO). The efficiency of (α-tocopherol + SSO) was like α-tocopherol and SSO used alone (Fig. 6B).

Nuclear factor (erythroid-derived 2)-like 2 (NRF2) is a transcription factor (T. Suzuki, J. Takahashi, M. Yamamoto, Molecular Basis of the KEAP1-NRF2 Signaling Pathway, Mol Cells 46, 2023). Under some oxidative stress conditions, NRF2, initially localized in the cytoplasm, can be phosphorylated on serine 40; this activated phosphorylated form translocates in the nuclei to increase the transcription of genes involved in oxidative stress response: Heme Oxygenase (HMOX), Mn-superoxide dismutase 2 (SOD2), and catalase (Francisqueti-Ferron et al., 2019; Reichard et al., 2007). On 158N cells, the (P-NRF2 (ser40)/NRF2) ratio, indicating an activation of the transcription factor was increased around 10 times in the presence of 7KC (Fig. 6C and D). OA, SSO and α-tocopherol normalized this activation (Fig. 6C and D). On 158N cells, in agreement, with the activation of NRF2, the use of RT-qPCR revealed an increased level of the mRNA levels of catalase, HMOX, SOD2 and catalase in the presence of 7KC (Fig. 6E – G). These effects were strongly attenuated when 7KC was associated with ALA, EPA, DHA, OA, SSO, Lorenzo's oil and α-tocopherol whereas EA was inefficient (Fig. 6E – G).

Incidence of α-linolenic acid, eicosapentaenoic acid, docosahexaenoic acid, oleic acid, erucic acid, Lorenzo's oil and sulpho-N-succinimidyl oleate without or with 7-ketocholesterol-on lipid droplets accumulation and on the intracellular accumulation of 7-ketocholesterol.

On 158N and ARPE-19 cells, the use of unsaturated FAs (ALA, EPA, DHA, EA and OA) and SSO as well as of Lorenzo's oil led us to specify the incidence of these compounds on the formation of lipid droplets. On 158N cells, lipid droplet formation was evaluated and quantified with Oil Red O (ORO; brightfield microscopy), and with Bodipy 493/503 (fluorescence microscopy; flow cytometry). ORO and Bodipy 493/503 stain in visible red and green fluorescence the neutral lipids present in lipid droplets, respectively. Different effects were observed on intracellular lipid droplets accumulation with the different unsaturated FAs (ALA, EPA, DHA, EA and OA), Lorenzo's oil, SSO and α-tocopherol. On 158N cells stained with ORO, a more or less pronounced accumulation of lipid droplets (red dots) was observed with ALA, EPA, DHA, OA and Lorenzo's oil; the highest quantities of lipid droplets per cell were observed with OA and Lorenzo's oil whereas only few cells with lipid droplets were observed in the presence of α-tocopherol, EA and SSO (Supplementary Fig. 3). Using brightfield microscopy, as ORO staining does not permit an accurate quantification of lipid droplets per cell, the lipid droplets were stained with Bodipy 493/503, and flow cytometric analyses were further realized (Fig. 7A and B). On 158N, by fluorescence microscopy, the visualization of lipid droplets with Bodipy 493/503 leads to similar conclusions that with ORO: lipid droplets (green fluorescent dots) were observed with ALA, EPA, DHA, OA and Lorenzo's oil; the highest quantities per cell were observed with OA and Lorenzo's oil whereas only few cells with lipid droplets were observed with α-tocopherol, EA and SSO (Fig. 7A and B). With 7KC, few lipid droplets were detected with ORO (Supplementary Fig. 3) and Bodipy 493/503 (Fig. 7B). On 158N cells, the data obtained by fluorescence microscopy agreed with flow cytometric analyses: a significant increase of the ratio [Mean Fluorescence Intensity (MFI) assay/MFI control] was only observed with OA and Lorenzo's oil. With 7KC, a slight but not significant increase of the MFI ratio was found; no significant differences were identified between control, vehicle-treated cells and 7KC-treated cells. When 7KC was associated with ALA, EPA, and DHA, marked accumulation of lipid droplets was observed; the highest levels of lipid droplets

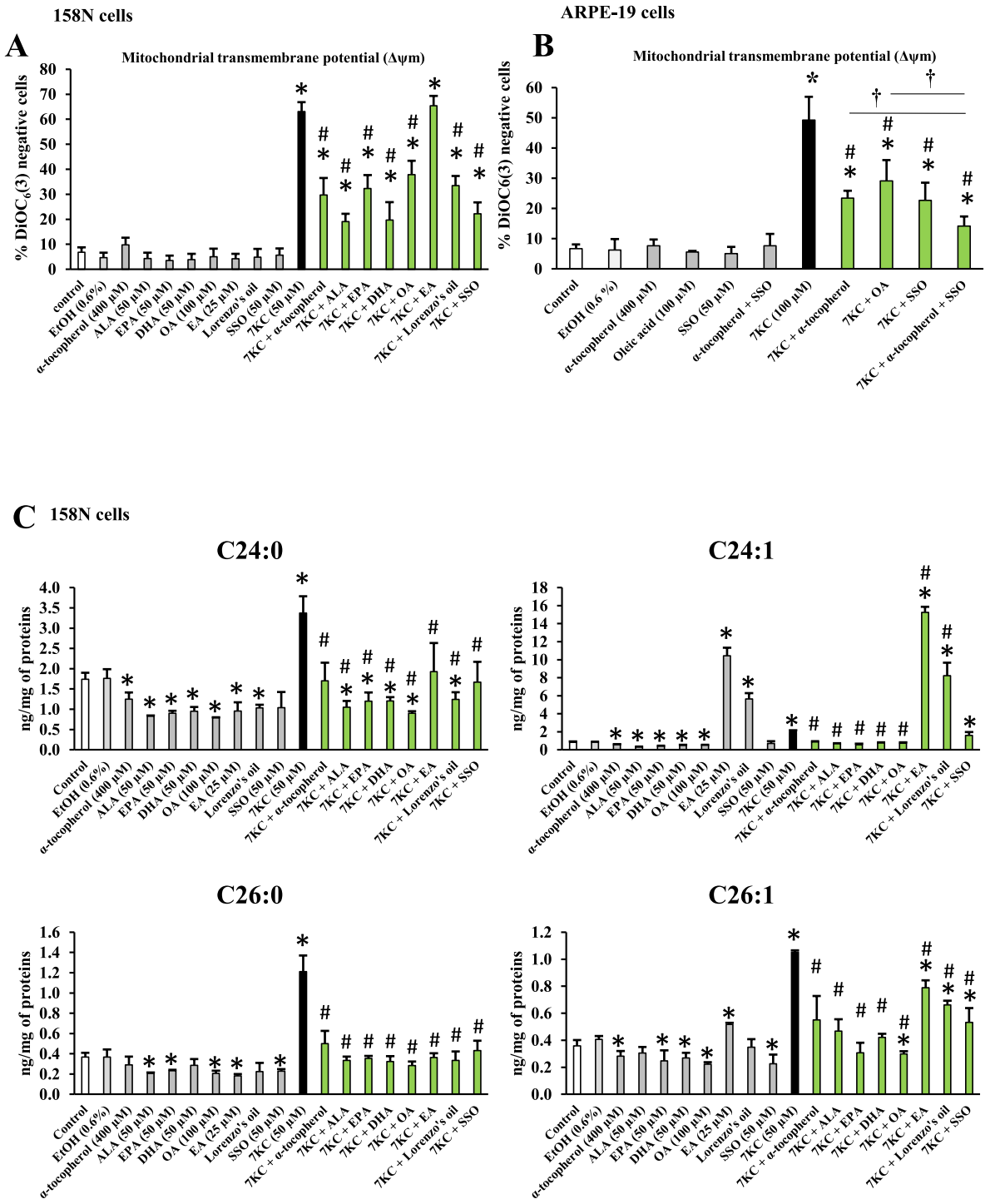

Fig. 4. Evaluation of the effects of α-linolenic acid, eicosapentaenoic acid, docosahexaenoic acid, oleic acid, erucic acid, sulfo-N-succinimidyl oleate and Lorenzo's oil on 7-ketocholestel-induced mitochondrial and peroxisomal dysfunction. 158N and ARPE-19 cells previously cultured for 24 h were further incubated for a 24 h additional period of time with 7-ketocholesterol, FAs (α-linolenic acid (ALA), eicosapentaenoic acid (EPA), docosahexaenoic acid (DHA), oleic acid (OA), erucic acid (EA)), sulfo-N-succinimidyl oleate (SSO), or Lorenzo's oils (OA + EA; 4:1) as well as α-tocopherol (reference cytoprotective molecule) and with 7KC associated with ALA, EPA, DHA, OA, EA, SSO, Lorenzo's oil or α-tocopherol. Mitochondrial dysfunction was evaluated by the percentage of cells with altered mitochondria characterized by a loss of ΔΨm (this parameter was determined by flow cytometry after staining with $DiOC_6(3)$) (**A** 158N cells**; B** ARPE-19 cells). Peroxisomal dysfunction was studied on 158N cells; it was estimated by the levels of VLCFAs (C24:0, C24:1, C26:0, C26:1) measured by GC–MS (**C**). Data are expressed as mean ± standard deviation (SD) of three independent experiments performed in triplicate. Significance of the differences between control (untreated cells) and EtOH (0.6 %), ALA, EPA, DHA, OA, EA, SSO, Lorenzo's oil, or α-tocopherol-treated cells, 7KC and (7KC + (ALA, EPA, DHA, OA, EA, SSO, Lorenzo's oil, or α-tocopherol)); Mann Whitney test: * $P \leq 0.05$. Significance of the differences between 7KC-treated cells and (7KC + (ALA, EPA, DHA, OA, EA, SSO, Lorenzo's oil or α-tocopherol)-treated cells; Mann Whitney test: # $P \leq 0.05$. Significance of the differences between (7KC + α-tocopherol + SSO) and (7KC + α-tocopherol) or (7KC + SSO) † $P \leq 0.05$. No significant differences were observed between control (untreated cells) and vehicle control (Ethanol (EtOH) 0.6 %).

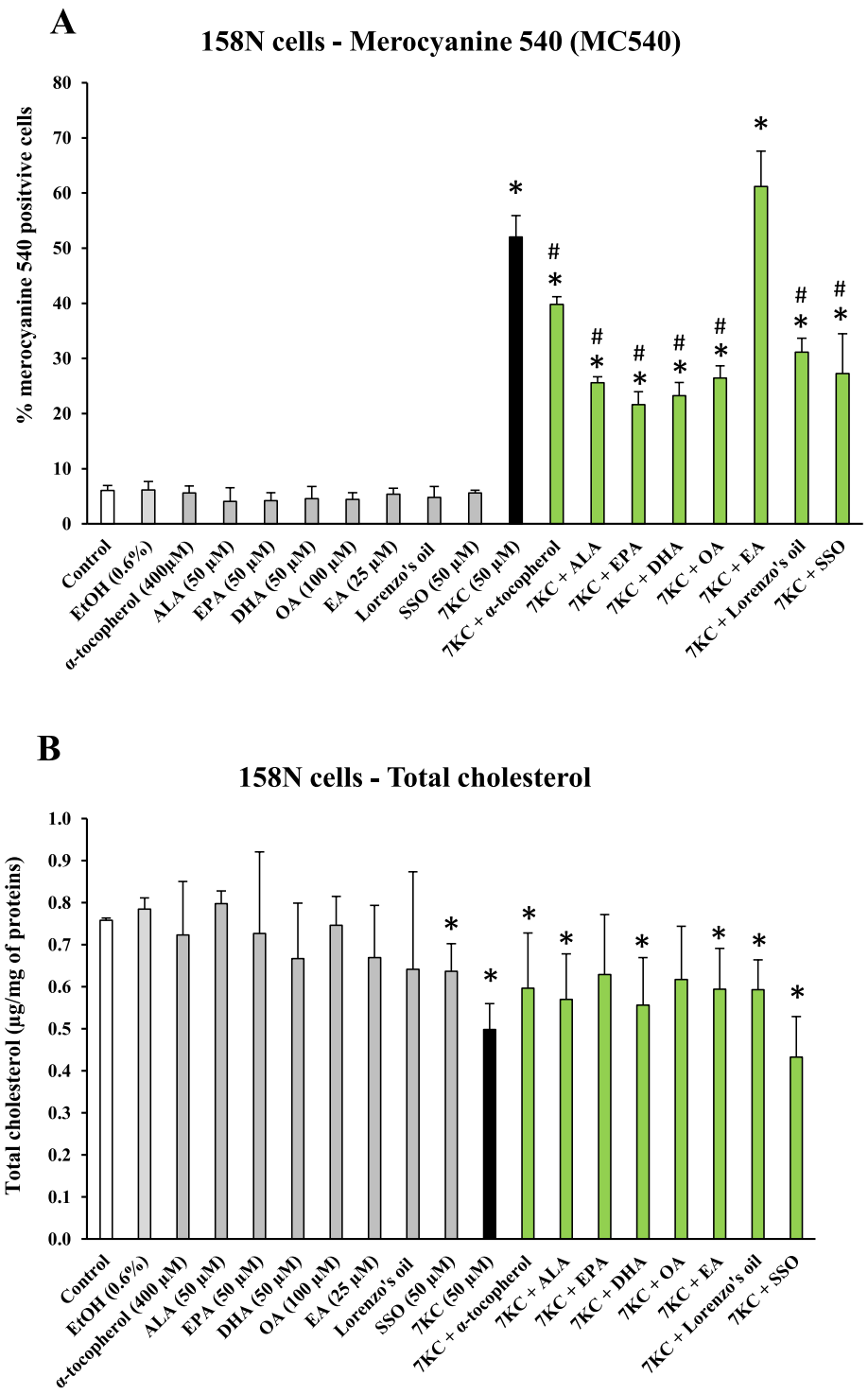

Fig. 5. Effects of α-linolenic acid, eicosapentaenoic acid, docosahexaenoic acid, oleic acid, erucic acid, Lorenzo's oil and sulpho-N-succinimidyl oleate on 7-ketocholesterol-induced plasma membrane lipid disorganization. 158N cells previously cultured for 24 h were further incubated for a 24 h additional period of time with 7-ketocholesterol (7KC; 50 µM), FAs (α-linolenic acid (ALA), eicosapentaenoic acid (EPA), docosahexaenoic acid (DHA), oleic acid (OA), erucic acid (EA)), sulfo-N-succinimidyl oleate (SSO), or Lorenzo's oils (OA + EA; 4:1) as well as α-tocopherol (reference cytoprotective molecule) and with 7KC associated with ALA, EPA, DHA, OA, EA, SSO, Lorenzo's oil or α-tocopherol. At the end of the treatment, the percentage of MC540 positive cells was determined by flow cytometry (**A**), and the total cholesterol content was quantified by GC–MS (**B**). Data are expressed as mean ± standard deviation (SD) of three independent experiments performed in triplicate. Significance of the differences between control (untreated cells) and EtOH (0.6 %), ALA, EPA, DHA, OA, EA, SSO, Lorenzo's oil, α-tocopherol-treated cells, 7KC and (7KC + (ALA, EPA, DHA, OA, EA, SSO, Lorenzo's oil, or α-tocopherol)); Mann Whitney test: * $P \leq 0.05$. Significance of the differences between 7KC-treated cells and (7KC + (ALA, EPA, DHA, OA, EA, SSO, Lorenzo's oil or α-tocopherol)-treated cells; Mann Whitney test: # $P \leq 0.05$. No significant differences were observed between control (untreated cells) and vehicle control (Ethanol (EtOH) 0.6 %).

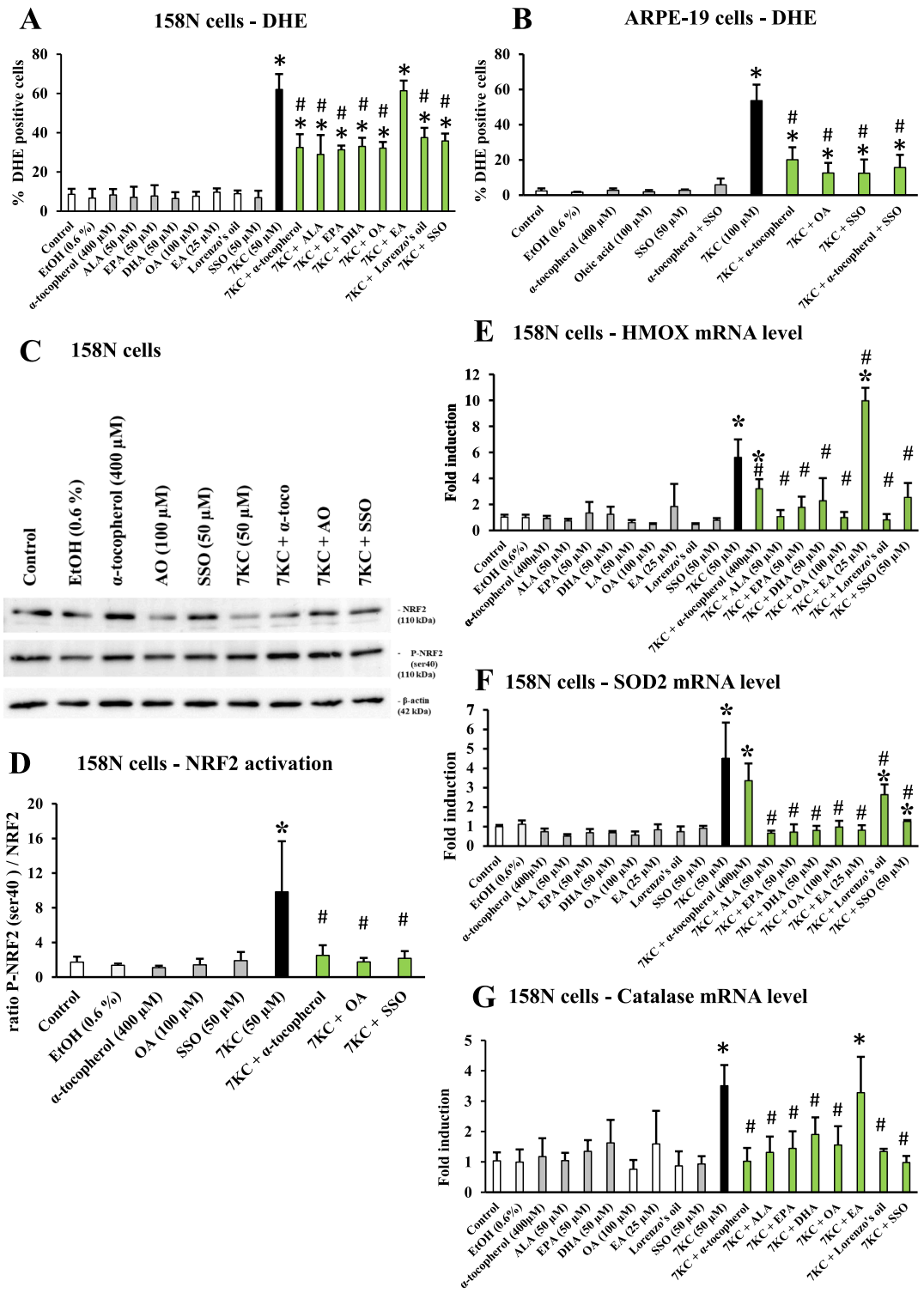

Fig. 6. Evaluation of the effects of α-linolenic acid, eicosapentaenoic acid, docosahexaenoic acid, oleic acid, Lorenzo's oil and sulpho-N-succinimidyl oleate associated or not with 7-ketocholesterol on oxidative stress. 158N and ARPE-19 cells previously cultured for 24 h were further incubated for a 24 h additional period of time with 7-ketocholesterol, FAs (α-linolenic acid (ALA), eicosapentaenoic acid (EPA), docosahexaenoic acid (DHA), oleic acid (OA), erucic acid (EA)), sulfo-N-succinimidyl oleate (SSO), or Lorenzo's oils (OA + EA; 4:1) as well as α-tocopherol (reference cytoprotective molecule) and with 7KC associated with ALA, EPA, DHA, OA, EA, SSO, Lorenzo's oil or α-tocopherol. At the end of the treatment, the percentage of ROS overproducing cells was determined by flow cytometry after staining with DHE (**A** 158N cells; **B** ARPE-19 cells). NRF2 activation was determined by western blotting on 158N cells using the (P-NRF2 (ser40)/ NRF2) ratio (**C**, **D**). 158N cells mRNA levels of HMOX (**E**), SOD2 (**F**) and catalase (**G**) were quantified by RT-qPCR. Data are expressed as mean ± standard deviation (SD) of three independent experiments performed in triplicate. Significance of the differences between control (untreated cells) and EtOH (0.6 %), ALA, EPA, DHA, OA, EA, SSO, Lorenzo's oil, α-tocopherol-treated cells, 7KC and (7KC + (ALA, EPA, DHA, OA, EA, SSO, Lorenzo's oil, or α-tocopherol)); Mann Whitney test: * $P \leq 0.05$. Significance of the differences between 7KC-treated cells and (7KC + (ALA, EPA, DHA, OA, EA, SSO, Lorenzo's oil or α-tocopherol)-treated cells; Mann Whitney test: # $P \leq 0.05$. Significance of the differences between (7KC + α-tocopherol + SSO) and (7KC + α-tocopherol) or (7KC + SSO); † $P \leq 0.05$. No significant differences were observed between control (untreated cells) and vehicle control (Ethanol (EtOH) 0.6 %).

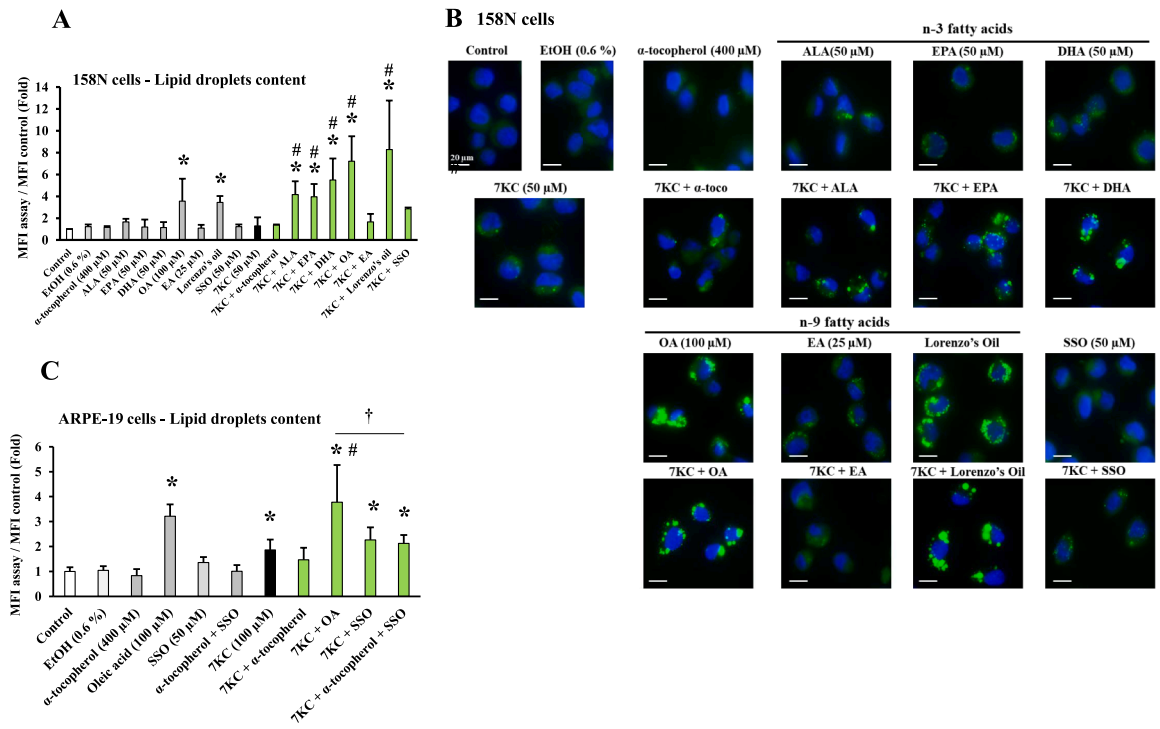

Fig. 7. Evaluation of the effects of α-linolenic acid, eicosapentaenoic acid, docosahexaenoic acid, oleic acid, erucic acid, Lorenzo's oil and sulpho-N-succinimidyl oleate associated or not with 7-ketocholesterol-on lipid droplets accumulation measured with Bodipy 493/503. 158N and ARPE-19 cells previously cultured for 24 h were further incubated for a 24 h additional period of time with 7-ketocholesterol, FAs (α-linolenic acid (ALA), eicosapentaenoic acid (EPA), docosahexaenoic acid (DHA), oleic acid (OA), erucic acid (EA)), sulfo-N-succinimidyl oleate (SSO), or Lorenzo's oils (OA + EA; 4:1) as well as α-tocopherol (reference cytoprotective molecule) and with 7KC associated with ALA, EPA, DHA, OA, EA, SSO, Lorenzo's oil or α-tocopherol. At the end of the treatment, the cells were stained with Bodipy 493/503. The green fluorescence of Bodipy 493/503 was quantified by flow cytometry on 158N cells (**A**) and ARPE-19 cells (**C**); data were expressed as MFI ratio [MFI assay/MFI control]. 158N cells were also observed by fluorescence microscopy (**B**). Data are expressed as mean ± standard deviation (SD) of three independent experiments performed in triplicate. Significance of the differences between control (untreated cells) and EtOH (0.6 %), ALA, EPA, DHA, OA, EA, SSO, Lorenzo's oil, α-tocopherol-treated cells, 7KC and (7KC + (ALA, EPA, DHA, OA, EA, SSO, Lorenzo's oil, or α-tocopherol)); Mann Whitney test: * $P \leq 0.05$. Significance of the differences between 7KC-treated cells and (7KC + (ALA, EPA, DHA, OA, EA, SSO, Lorenzo's oil or α-tocopherol)-treated cells; Mann Whitney test: # $P \leq 0.05$. Significance of the differences between 7KC + α-tocopherol + SSO and 7KC + α-tocopherol or 7KC + SSO † $P \leq 0.05$. No significant differences were observed between control (untreated cells) and vehicle control (Ethanol (EtOH) 0.6 %). (For interpretation of the references to colour in this figure legend, the reader is referred to the web version of this article.)

per cell were observed with (7KC + OA) and (7KC + Lorenzo's oil) whereas no lipid droplets accumulation was detected when 7KC was associated with EA, SSO and α-tocopherol (Fig. 7).

On ARPE-19 cells, lipid droplet formation was only evaluated by flow cytometry after staining with Bodipy 493/503 (Fig. 7C). OA induced an increase accumulation of lipid droplets per cell; no effects were observed with SSO or α-tocopherol alone or with (α-tocopherol + SSO) (Fig. 7C). Comparatively to untreated cells and vehicle-treated cells, 7KC induced a slight but significant accumulation of lipid droplets which was strongly and significantly amplified in the presence of OA, and not significantly modified with α-tocopherol, SSO or (α-tocopherol + SSO) (Fig. 7C).

On 158N cells, we also asked whether unsaturated fatty acids (ALA, EPA, DHA, OA, EA), Lorenzo'oil, SSO and α-tocopherol, reduced the cellular accumulation of 7KC. On 158N cells, intracellular accumulations of 7KC and unsaturated FAs were observed (Supplementary Fig. 4). 7KC accumulation was significantly decreased with the different compounds used, excepted with OA (Supplementary Fig. 4).

Prevention of 7KC-induced apoptosis and autophagy with ω3 fatty acids (α-linolenic acid, eicosapentaenoic acid, docosahexaenoic acid) and sulpho-N-succinimidyl oleate on 158N cells.

The results obtained on 158N cells suggest that the destabilization of plasma membrane lipid organization evaluated with MC540 could be an early event leading to several cellular dysfunctions leading to a drop in ΔΨm (Vejux et al., 2009). On 158N cells, 7KC-induced cell death was associated with a decreased level of Mcl-1 linked with an increased level of P-Mcl-1 (Ser159/Thr163) as well as with a strong increase of the ratio Bad/Mcl-1 (Fig. 8). These data support the hypothesis that the increase in P-Mcl-1 (Ser159/Thr163) leads to an inhibition of Bad sequestration in the cytoplasm thus favoring its interaction with the mitochondrial membrane to induce the drop of ΔΨm (Ragot et al., 2011). 7KC-induced cell death was also associated with a caspase-3 cleavage leading to an activation of this enzyme which contributes to PARP degradation supporting an activation of apoptosis (Fig. 8). The ability of Z-VAD-fmk (a pan-caspases inhibitor) to strongly inhibit 7KC-induced cell death, demonstrates an active contribution of apoptosis in 7KC-induced cell death on 158N cells (Supplementary Fig. 5). In addition, in the presence of 7KC, an activation of LC3-I into LC3-II, which is an autophagic criteria, was observed (Fig. 8). 7KC-induced autophagy on 158N cells can be considered as survival autophagy because cell death decreased in the presence of rapamycin (an autophagy activator) and increased in the presence of 3-methyladenine (an autophagy inhibitor) (Supplementary Fig. 5). When 7KC was combined with FAs (ALA, EPA, DHA) or SSO, as well as with α-tocopherol, the induction of apoptosis and autophagy was strongly reduced (Fig. 8). No pro-apoptototic and pro-autophagic effects were observed when ALA, EPA, DHA, SSO and α-tocopherol were used alone (Fig. 8). These results obtained on 158N cells demonstrate the ability of FAs (ALA, EPA, DHA), SSO, and α-tocopherol to prevent mitochondrial depolarization and to counteract the induction of cell death by apoptosis as well as the activation of autophagy.

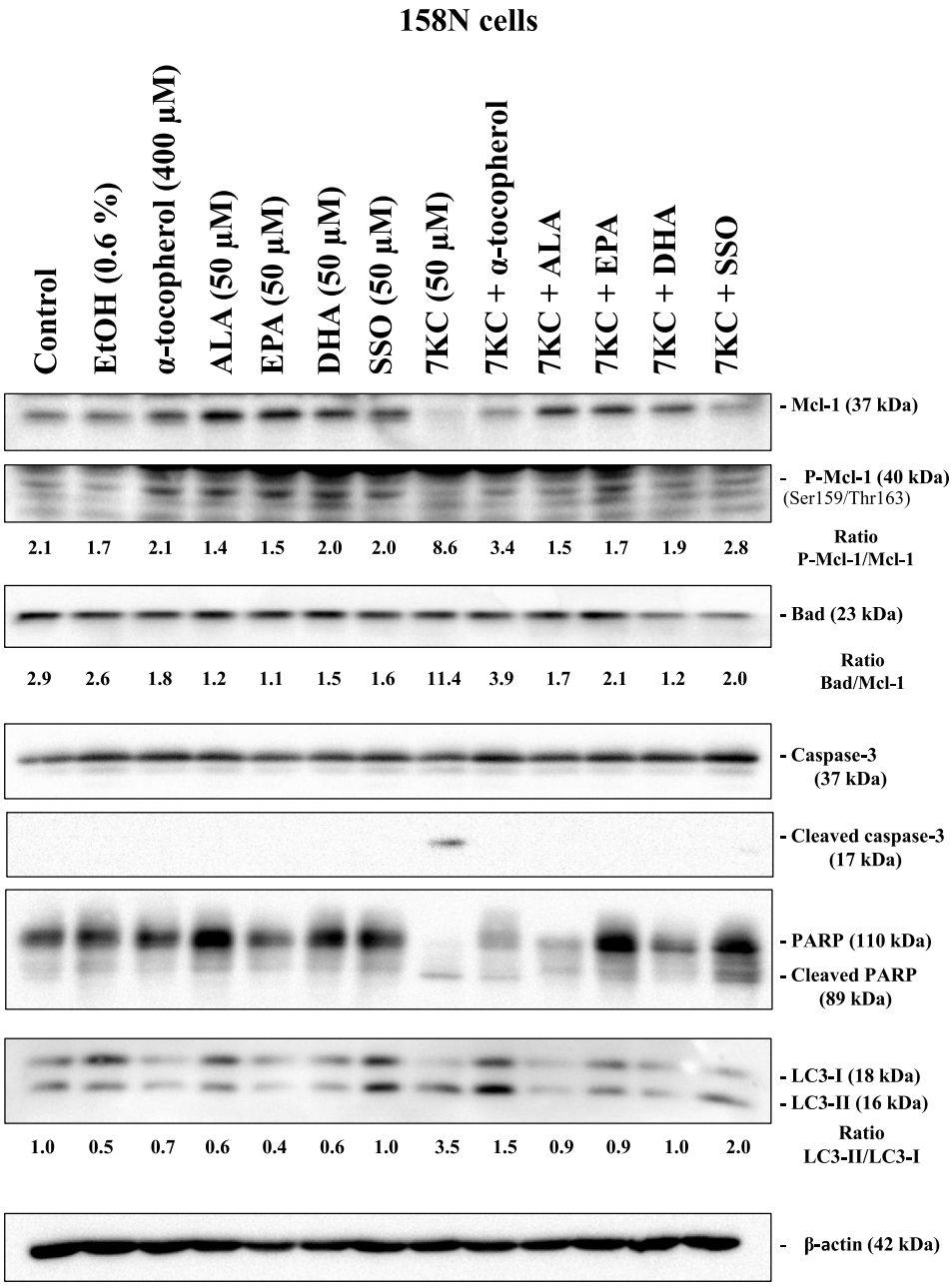

Fig. 8. Evaluation of the effects of α-linolenic acid, eicosapentaenoic acid, docosahexaenoic acid, oleic acid, Lorenzo's oil and sulpho-N-succinimidyl oleate associated or not with 7-ketocholesterol on apoptosis and autophagy. Apoptosis and autophagy were characterized by Western blotting with different antibodies. Apoptosis was evaluated by Mcl-1, P-Mcl-l (Ser159/Thr163) and Bad levels, [Bad/Mcl-1] ratio, caspase-3 activation (cleaved caspase-3), and PARP degradation, and autophagy by conversion of LC3-I to LC3-II [ratio LC3-II/LC3-I].

Discussion

7KC-induced cytotoxic effects including plasma membrane alterations, organelle dysfunctions, and ROS overproduction triggering cell death associated or not with inflammation (Vejux et al., 2020). To counteract these cytotoxic effects induced by 7KC, which is often present at increased level in patients with age related diseases such as cardiovascular diseases, ocular diseases (AMD, cataract) and neurodegenerative diseases (mainly Alzheimer's disease) (Zarrouk et al., 2014; Anderson et al., 2020), the identification of natural or synthetic molecules or of mixtures of molecules targeting the signaling pathways involved in 7KC-induced cytotoxicity is a major challenge (Nury et al., 2021). In the present study, we showed that ω-3 and ω-9 FAs (ALA, EPA, DHA, OA), Lorenzo's oil, and sulfo-N-succinimidyl oleate (SSO), a synthetic analogue of OA, attenuate the toxicity of 7KC. On 158N oligodendrocytes, these compounds strongly reduced 7KC-induced plasma membrane disorganization, oxidative stress, mitochondrial and peroxisomal dysfunction, as well as oxiapoptophagy, which is a caspase-dependent mode of cell death associated with oxidative stress and autophagy (Nury et al., 2020). On retinal epithelial ARPE19 cells, these different compounds also strongly reduced 7KC-induced oxidative stress, mitochondrial dysfunction, ROS overproduction, and cell death (Dugas et al., 2010). Noteworthy, among the different compounds studied, SSO as well as α-tocopherol (used as reference cytoprotective molecule) were the only compounds preventing the toxicity of 7KC without simultaneous accumulation of lipid droplets.

Currently, little is known about the mechanisms associated with the cytoprotection of FAs. However, it must be underlined that among the

FAs tested (ALA, EPA, DHA, OA and EA), only EA is not cytoprotective, and does not prevent 7KC-induced cell death. The ability of ALA, EPA, DHA and OA to prevent 7KC-induced plasma membrane disorganization was demonstrated in our study on 158N cells using MC540 and cholesterol quantification. As the same FAs (ALA, EPA, DHA and OA) reduce 7KC-induced ROS overproduction revealed with DHE, both on 158N and ARPE-19 cells, it is suggested that plasma membrane alteration revealed with MC540 and observed in the presence of 7KC could be, at least in part, the consequence of lipid peroxidation. On U937 cells, 7KC-induced apoptosis associated with increased plasma membrane permeability was also associated with modification of free cholesterol level revealed by flow cytometry after staining with filipin (Vejux et al., 2005). The lack of cytoprotection with EA could be due to the possible irreversible interactions of this fatty acid with mitochondrial cardiolipins and to changes in the phosphatidyl choline/phosphatidylethanolamine ratio at the inner membrane of the mitochondria resulting in increased mitochondrial sensitivity to toxic agents (Bozcali et al., 2009). On the basis of results obtained with OA (Monier et al., 2003), the hypothesis that esterification of cholesterol with FAs would reduce the toxicity of 7KC is therefore not applicable to all FAs. It can be hypothesized that ALA, EPA, DHA and OA, by modifying the plasma membrane phospholipid composition, could counteract the insertion of 7KC into lipid rafts, as α-tocopherol does (Royer et al., 2009; Ragot et al., 2011), and restore cell signaling from the plasma membrane that helps preserve mitochondrial functionality. According to this hypothesis, based on the results obtained on U937 cells (Vejux et al., 2009), it can be thought that the functionality of the PIP3/PDK1/Akt signaling pathway connected with GSK3 (Ragot et al., 2011) and downregulated by 7KC (Brahmi et al., 2019; Vejux et al., 2009), could be restored by FAs thus promoting Mcl-1/Bad interactions and the sequestration of the latter in the cytoplasm: these effects would then contribute to repress 7KC-induced mitochondrial depolarization and to inhibit apoptosis. These data bring new elements supporting the essential role of the reactivation of the PIP3/PDK1/Akt signaling pathway in cell rescue (Yammine et al., 2024). Concerning DHA, in addition to being an important acyl chain of membrane phospholipids, it could also have cytoprotective activities thanks to biologically active derivatives such as neuroprotectin D1 (NPD1) which is an apoptosis inhibitor (Asatryan and Bazan, 2017). This emphasizes that the ability of DHA, like other FAs (ALA, EPA and OA), to prevent mitochondrial dysfunction is a key factor in inhibiting 7KC-induced apoptosis as well autophagy. These data agree with those obtained on 158N cells (Nury et al., 2015) and on N2a cells (Yammine et al., 2020). On ARPE-19 cells, it has been reported that DHA can both induce endogenous antioxidant activities and mobilizes selective autophagy of misfolded proteins (Johansson et al., 2015). On DHA-treated HepG2 cells, an induction of autophagy resulting from ROS overproduction has also been described (Mei et al., 2011). As survival autophagy has been described with 7KC as well as with 7β-OHC, the mechanisms by which survival autophagy induced by toxic oxysterols could protect against cell death are not yet understood, and could involve multiple mechanisms: recycling of misfolded and aggregated proteins, removing altered organelles (mitophagy, pexophagy) (Ghzaiel et al., 2022) and regulating fatty acid-induced lipid accumulation (lipophagy) to prevent lipotoxicity (Klionsky et al., 2016; Mei et al., 2011).

As a significant increase in the plasma level of 7KC was observed in X-ALD patients (Nury et al., 2017), this led us to evaluate the effects of Lorenzo's oil sometimes prescribed to X-ALD patients, in order to assess its cytoprotective activity. Lorenzo's oil (OA + EA; 4:1) is used to reduce the saturated VLCFA level (C26:0, C24:0) in X-ALD; however, its mechanism still remains elusive (Moser et al., 2007). EA and OA inhibit ELOVL1 enzyme (the primary enzyme responsible for the synthesis of saturated VLCFAs), and in this context the 4:1 mixture exhibits the most potent inhibitory activity. In addition, at the cellular level, treatment with the 4:1 mixture reduced the level of sphingomyelin with a saturated VLCFA (Sassa et al., 2014). The ability of Lorenzo's oil to inhibit 7KC-induced oxiapotophagy underscores its ability to inhibit ROS overproduction and cell death induced by this oxysterol. It should be noted that the effects on these parameters are due to OA and not EA. These new elements on the cytoprotective activity of Lorenzo's oil make it possible to envisage its use in patients other than X-ALD in whom increased levels of 7KC are observed.

In the present study, the most original results with important potential therapeutic applications have been obtained with the SSO. Indeed, this molecule deriving from OA, unlike ALA, EPA, DHA, and EA, is non-toxic over a wide range of concentrations (100 to 400 μM). The cytoprotective effects of SSO against 7KC are potent as demonstrated by its ability to reduce 7KC-induced lipid membrane disorganization, mitochondrial and peroxisomal dysfunction, overproduction of ROS, apoptosis, and autophagy. Furthermore, unlike other cytoprotective FAs (ALA, EPA, DHA and OA), SSO does not induce the accumulation of lipid droplets, which is a major advantage when considering further therapeutic applications. Despite these marked differences with FAs (ALA, EPA, DHA and OA), SSO similarly prevents plasma membrane damages and restores the signaling pathway implicating Mcl-1 that prevents the loss of ΔΨm leading to apoptosis. In addition, our data support that 7KC induced ROS overproduction initiates an NRF2 response which in turn activates the transcription of antioxidant enzymes, HMOX, SOD2 and catalase on 158N cells. We report that the cytoprotective lipid compounds as well as SSO enable the activation of signaling pathways that restore ΔΨm by acting on mitochondrial interaction proteins (Mcl-1, Bad) to prevent cell death. Compared to the natural and synthetic molecules already identified to inhibit the toxicity of 7KC (Brahmi et al., 2019; Cilla et al., 2017; Yammine et al., 2020), this study brings new elements and shows that FAs (ALA, EPA, DHA and OA), a mixture of FAs (Lorenzo's oil: OA and EA in a ratio 4:1) and SSO are powerful cytoprotectors: they prevent 7KC-induced plasma membrane disorganization, organelle dysfunction, loss of ΔΨm, apoptosis, and autophagy. However, among these lipids, SSO is the most promising compound: its non-toxic cytoprotective activities over a wide range of concentrations are not associated with cytoplasmic accumulation of lipid droplets. In addition, SSO is also able to protect against 24S-OHC- and Triol-induced cell death also considered to play key roles in age-related diseases (Samadi et al., 2021; Mahalakshmi et al., 2021; Poli et al., 2013).

Conclusions

In conclusion, SSO is a novel synthetic molecule, analogous to oleic acid (Coort et al., 2002; Harmon et al., 1991), that can be used to counter the toxicity of 7KC. Like three other synthetic molecules currently described, namely dimethyl fumarate (DMF), known as Tecfidera, monomethylfumarate (MMF) (Zarrouk et al., 2017) and UDP-003 (Bhargava et al., 2023), SSO opposes oxidative stress and cell death induced by 7KC associated with a drop of ΔΨm without causing a simultaneous accumulation of lipid droplets. In addition, SSO inhibits cell death induced by 7KC on 158N and ARPE-19 cells, while normalizing autophagy; moreover, SSO opposes peroxisomal metabolic dysfunctions which is not currently described with DMF, MMF and UDP-003. Serious hope can be based on SSO, especially since this molecule has already shown pharmacological activities in rats on models of metabolic diseases (Coort et al., 2002; Mansor et al., 2017). Thus, SSO has several attractive characteristics that make it a potential drug candidate to treat age-related diseases that are associated with increased levels of 7KC.

For G. Lizard and A.G. Atanasov: The author is an Editorial Board Member/Editor-in-Chief/Associate Editor/Guest Editor for [Journal name] and was not involved in the editorial review or the decision to publish this article.

CRediT authorship contribution statement

Thomas Nury: Validation, Investigation, Writing – original draft, Visualization. **Imen Ghzaiel:** Writing – review & editing. **Aziz**

Hichami: Conceptualization, Investigation. **Claudio Caccia:** Investigation. **Valerio Leoni:** Investigation. **Vivien Pires:** Investigation. **Atanas G Atanasov:** Writing – review & editing. **Amira Zarrouk:** Writing – review & editing. **Gérard Lizard:** Conceptualization, Methodology, Validation, Writing – original draft, Visualization, Supervision, Funding acquisition. **Anne Vejux:** Conceptualization, Methodology, Validation, Writing – original draft, Visualization, Supervision.

Declaration of competing interest

The authors declare that they have no known competing financial interests or personal relationships that could have appeared to influence the work reported in this paper.

Data availability

No data was used for the research described in the article.

Acknowledgements

This work was presented in Thomas Nury's thesis manuscript, supervised by Dr Gérard Lizard and Dr Anne Vejux and entitled "Modifications peroxysomales associées à l'oxyapoptophagie induite par le 7-cétocholestérol et identification de lipides cytoprotecteurs" (presented and defended in Dijon on December 3, 2020). This work was presented by Thomas Nury (Ph.D) as a poster at the 9th ENOR Symposium "Metabolism and Oxysterols: Therapeutics for Lifelong Health", September 19-20, 2019, University of Edinburgh, Edinburgh, Scotland (UK) (https://www.oxysterols.net/). This work was supported by grants from: Univ. Bourgogne (Dijon, France); SATT Sayens (Dijon, France), University Tunis El Manar (Tunis, Tunisia), University of Monastir (Monastir, Tunisia) and ABASIM (Association Bourguignonne pour les Applications des Sciences de l'Information en Médecine, Dijon, France). This work has benefited from the logistical support of the INPST network (International Natural Product Sciences Taskforce (INPST: https://inpst.net/); Prof A Atanasov, Dr G Lizard).

Appendix A. Supplementary data

Supplementary data to this article can be found online at https://doi.org/10.1016/j.crbiot.2024.100195.

References

Anderson, A., Campo, A., Fulton, E., Corwin, A., Jerome, W.G., O'Connor, M.S., 2020. 7-ketocholesterol in disease and aging. Redox Biol 29, 101380. https://doi.org/10.1016/j.redox.2019.101380.

Asatryan, A., Bazan, N.G., 2017. Molecular mechanisms of signaling via the docosanoid neuroprotectin D1 for cellular homeostasis and neuroprotection. J Biol Chem 292, 12390–12397.

Baarine, M., Ragot, K., Genin, E.C., El Hajj, H., Trompier, D., Andreoletti, P., 2009. Peroxisomal and mitochondrial status of two murine oligodendrocytic cell lines (158N, 158JP): potential models for the study of peroxisomal disorders associated with dysmyelination processes. J Neurochem 111, 119–131.

Baarine, M., Andréoletti, P., Athias, A., Nury, T., Zarrouk, A., Ragot, K., Vejux, A., Riedinger, J.-M., Kattan, Z., Bessede, G., Trompier, D., Savary, S., Cherkaoui-Malki, M., Lizard, G., 2012. Evidence of oxidative stress in very long chain fatty acid–treated oligodendrocytes and potentialization of ROS production using RNA interference-directed knockdown of ABCD1 and ACOX1 peroxisomal proteins. Neuroscience 213, 1–18. https://doi.org/10.1016/j.neuroscience.2012.03.058.

P. Bhargava, D. Dinh, F. Teramayi, A. Silberg, N. Petler, A.M. Anderson, D.M. Clemens, M.S. O'Connor, Selective Removal of 7KC by a Novel Atherosclerosis Therapeutic Candidate Reverts Foam Cells to a Macrophage-like Phenotype, bioRxiv (2023) 2023.10.23.563623. 10.1101/2023.10.23.563623.

Bjorkhem, I., Meaney, S., 2004. Brain cholesterol: long secret life behind a barrier. Arterioscler Thromb Vasc Biol 24, 806–815.

Bozcali, E., Süzer, O., Gürsoy, H.N., Atukeren, P., Gümüstas, K.M., 2009. Effects of erucic acid supplemented feeding on chronic doxorubucin toxicity in rats, international journal of. Clinical and Experimental Medicine 2, 337–347.

Brahmi, F., Vejux, A., Sghaier, R., Zarrouk, A., Nury, T., Meddeb, W., Rezig, L., Namsi, A., Sassi, K., Yammine, A., Badreddine, I., Vervandier-Fasseur, D., Madani, K., Boulekbache-Makhlouf, L., Nasser, B., Lizard, G., 2019. Prevention of 7-ketocholesterol-induced side effects by natural compounds. Crit Rev Food Sci Nutr 59, 3179–3198. https://doi.org/10.1080/10408398.2018.1491828.

Bresciani, G., Manai, F., Davinelli, S., Tucci, P., Saso, L., Amadio, M., 2023. Novel potential pharmacological applications of dimethyl fumarate-an overview and update. Front Pharmacol 14, 1264842. https://doi.org/10.3389/fphar.2023.1264842.

Brown, A.J., Jessup, W., 1999. Oxysterols and atherosclerosis. Atherosclerosis 142, 1–28.

Cilla, A., Alegría, A., Attanzio, A., Garcia-Llatas, G., Tesoriere, L., Livrea, M.A., 2017. Dietary phytochemicals in the protection against oxysterol-induced damage. Chem Phys Lipids 207, 192–205.

Cooper, R.A., 1978. Influence of increased membrane cholesterol on membrane fluidity and cell function in human red blood cells. Journal of Supramolecular Structure 8, 413–430.

Coort, S.L., Willems, J., Coumans, W.A., Vusse, G.J., Bonen, A., Glatz, J.F., 2002. Sulfo-N-succinimidyl esters of long chain fatty acids specifically inhibit fatty acid translocase (FAT/CD36)-mediated cellular fatty acid uptake. Molecular and Cellular Biochemistry 239, 213–219.

Debbabi, M., Zarrouk, A., Bezine, M., Meddeb, W., Nury, T., Badreddine, A., Karym, E. M., Sghaier, R., Bretillon, L., Guyot, S., Samadi, M., Cherkaoui-Malki, M., Nasser, B., Mejri, M., Ben-Hammou, S., Hammami, M., Lizard, G., 2017. Comparison of the effects of major fatty acids present in the Mediterranean diet (oleic acid, docosahexaenoic acid) and in hydrogenated oils (elaidic acid) on 7-ketocholesterol-induced oxiapoptophagy in microglial BV-2 cells. Chem Phys Lipids 207, 151–170. https://doi.org/10.1016/j.chemphyslip.2017.04.002.

Dhungana, H., Huuskonen, M.T., Jaronen, M., Lemarchant, S., Ali, H., Keksa-Goldsteine, V., 2017. Sulfosuccinimidyl oleate sodium is neuroprotective and alleviates stroke-induced neuroinflammation. Journal of Neuroinflammation 14, 237.

Doria, M., Nury, T., Delmas, D., Moreau, T., Lizard, G., Vejux, A., 2019. Protective function of autophagy during VLCFA-induced cytotoxicity in a neurodegenerative cell model. Free Radic Biol Med 137, 46–58. https://doi.org/10.1016/j.freeradbiomed.2019.04.016.

Drahota, Z., Vrbacky, M., Nuskova, H., Kazdova, L., Zidek, V., Landa, V., 2010. Succinimidyl oleate, established inhibitor of CD36/FAT translocase inhibits complex III of mitochondrial respiratory chain. Biochem Biophys Res Commun 391, 1348–1351.

Duc, D., Vigne, S., Pot, C., 2019. Oxysterols in autoimmunity. Int J Mol Sci 20, 4522.

Dugas, B., Charbonnier, S., Baarine, M., Ragot, K., Delmas, D., Ménétrier, F., Lherminier, J., Malvitte, L., Khalfaoui, T., Bron, A., Creuzot-Garcher, C., Latruffe, N., Lizard, G., 2010. Effects of oxysterols on cell viability, inflammatory cytokines, VEGF, and reactive oxygen species production on human retinal cells: cytoprotective effects and prevention of VEGF secretion by resveratrol. European Journal of Nutrition 49, 435–446. https://doi.org/10.1007/s00394-010-0102-2.

Francisqueti-Ferron, F.V., Ferron, A.J.T., Garcia, J.L., Silva, C.C.V. de A., Costa, M.R., Gregolin, C.S., Moreto, F., Ferreira, A.L.A., Minatel, I.O., Correa, C.R., 2019. Basic concepts on the role of nuclear factor erythroid-derived 2-like 2 (Nrf2) in age-related diseases. Int J Mol Sci 20, 3208. https://doi.org/10.3390/ijms20133208.

Ghosh, S., Ghzaiel, I., Vejux, A., Meaney, S., Nag, S., Lizard, G., Tripathi, G., Naez, F., Paul, S., 2024. Impact of oxysterols in age-related disorders and strategies to alleviate adverse effects. Adv Exp Med Biol 1440, 163–191. https://doi.org/10.1007/978-3-031-43883-7_9.

Ghzaiel, Sassi, Khouloud, A. Zarrouk, S. Ghosh, I.H.K. Dias, T. Nury, M. Ksila, S. Essadek, M. Tahri Joutey, F. Brahmi, W. Mihoubi, S. Rup-Jacques, M. Samadi, L. Rezig, S. Meziane, T. Ghrairi, O. Masmoudi-Kouki, S. Hammami, B. Nasser, M. Hammami, Y. Wang, W.J. Griffiths, A. Vejux, G. Lizard, Sources of 7-ketocholesterol, metabolism and inactivation strategies: food and biomedical applications, Redox Experimental Medicine Volume 2022: Issue 1 (n.d.) R40–R56.

Ghzaiel, I., Zarrouk, A., Essadek, S., Martine, L., Hammouda, S., Yammine, A., Ksila, M., Nury, T., Meddeb, W., Tahri Joutey, M., Mihoubi, W., Caccia, C., Leoni, V., Samadi, M., Acar, N., Andreoletti, P., Hammami, S., Ghrairi, T., Vejux, A., Hammami, M., Lizard, G., 2022. Protective effects of milk thistle (sylibum marianum) seed oil and α-tocopherol against 7β-hydroxycholesterol-induced peroxisomal alterations in murine C2C12 myoblasts: nutritional insights associated with the concept of pexotherapy. Steroids 183, 109032. https://doi.org/10.1016/j.steroids.2022.109032.

Ghzaiel, I., Maaloul, S., Ksila, M., Namsi, A., Yammine, A., Debbabi, M., Badreddine, A., Meddeb, W., Pires, V., Nury, T., Ménétrier, F., Avoscan, L., Zarrouk, A., Baarine, M., Masmoudi-Kouki, O., Ghrairi, T., Abdellaoui, R., Nasser, B., Hammami, S., Hammami, M., Samadi, M., Vejux, A., Lizard, G., 2024. In vitro evaluation of the effects of 7-ketocholesterol and 7β-hydroxycholesterol on the peroxisomal status: prevention of peroxisomal damages and concept of pexotherapy. Adv Exp Med Biol 1440, 437–452. https://doi.org/10.1007/978-3-031-43883-7_21.

Harmon, C.M., Luce, P., Beth, A.H., Abumrad, N.A., 1991. Labeling of adipocyte membranes by sulfo-N-succinimidyl derivatives of long-chain fatty acids: inhibition of fatty acid transport. J Membr Biol 121, 261–268. https://doi.org/10.1007/BF01951559.

Johansson, I., Monsen, V.T., Pettersen, K., Mildenberger, J., Misund, K., Kaarniranta, K., 2015. The marine n-3 PUFA DHA evokes cytoprotection against oxidative stress and protein misfolding by inducing autophagy and NFE2L2 in human retinal pigment epithelial cells. Autophagy 11, 1636–1651.

Klionsky, D.J., Abdelmohsen, K., Abe, A., Abedin, M.J., Abeliovich, H., Acevedo Arozena, A., 2016. Guidelines for the use and interpretation of assays for monitoring autophagy. Autophagy 12, 1–222.

Leoni, V., Nury, T., Vejux, A., Zarrouk, A., Caccia, C., Debbabi, M., Fromont, A., Sghaier, R., Moreau, T., Lizard, G., 2017. Mitochondrial dysfunctions in 7-ketocholesterol-treated 158N oligodendrocytes without or with α-tocopherol: impacts on the

cellular profil of tricarboxylic cycle-associated organic acids, long chain saturated and unsaturated fatty acids, oxysterols, cholesterol and cholesterol precursors. The Journal of Steroid Biochemistry and Molecular Biology 169, 96–110. https://doi.org/10.1016/j.jsbmb.2016.03.029.

Mahalakshmi, K., Parimalanandhini, D., Sangeetha, R., Livya Catherene, M., Beulaja, M., Thiagarajan, R., Arumugam, M., Janarthanan, S., Manikandan, R., 2021. Influential role of 7-ketocholesterol in the progression of alzheimer's disease. Prostaglandins Other Lipid Mediat 156, 106582. https://doi.org/10.1016/j.prostaglandins.2021.106582.

Mansor, L.S., Sousa Fialho, M. da L., Yea, G., Coumans, W.A., West, J.A., Kerr, M., Carr, C.A., Luiken, J.J.F.P., Glatz, J.F.C., Evans, R.D., Griffin, J.L., Tyler, D.J., Clarke, K., Heather, L.C., 2017. Inhibition of sarcolemmal FAT/CD36 by sulfo-N-succinimidyl oleate rapidly corrects metabolism and restores function in the diabetic heart following hypoxia/reoxygenation. Cardiovasc Res 113, 737–748. https://doi.org/10.1093/cvr/cvx045.

Mathieu, J., Schloendorn, J., Rittmann, B.E., Alvarez, P.J., 2008. Microbial degradation of 7-ketocholesterol. Biodegradation 19, 807–813.

Mei, S., Ni, H.M., Manley, S., Bockus, A., Kassel, K.M., Luyendyk, J.P., 2011. Differential roles of unsaturated and saturated fatty acids on autophagy and apoptosis in hepatocytes. J Pharmacol Exp Ther 339, 487–498.

Monier, S., Samadi, M., Prunet, C., Denance, M., Laubriet, A., Athias, A., Berthier, A., Steinmetz, E., Jürgens, G., Nègre-Salvayre, A., Bessède, G., Lemaire-Ewing, S., Néel, D., Gambert, P., Lizard, G., 2003. Impairment of the cytotoxic and oxidative activities of 7 beta-hydroxycholesterol and 7-ketocholesterol by esterification with oleate. Biochem Biophys Res Commun 303, 814–824. https://doi.org/10.1016/s0006-291x(03)00412-1.

Moser, H.W., Moser, A.B., Hollandsworth, K., Brereton, N.H., Raymond, G.V., 2007. Lorenzo's oil" therapy for X-linked adrenoleukodystrophy: rationale and current assessment of efficacy. Journal of Molecular Neuroscience : MN 33, 105–113.

Mutemberezi, V., Guillemot-Legris, O., Muccioli, G.G., 2016. Oxysterols: from cholesterol metabolites to key mediators. Prog Lipid Res 64, 152–169. https://doi.org/10.1016/j.plipres.2016.09.002.

Namsi, A., Nury, T., Hamdouni, H., Yammine, A., Vejux, A., Vervandier-Fasseur, D., Latruffe, N., Masmoudi-Kouki, O., Lizard, G., 2018. Induction of neuronal differentiation of murine N2a cells by two polyphenols present in the Mediterranean diet mimicking neurotrophins activities: resveratrol and apigenin. Diseases 6, E67. https://doi.org/10.3390/diseases6030067.

Namsi, A., Nury, T., Khan, A.S., Leprince, J., Vaudry, D., Caccia, C., Leoni, V., Atanasov, A.G., Tonon, M.-C., Masmoudi-Kouki, O., Lizard, G., 2019. Octadecaneuropeptide (ODN) induces N2a cells differentiation through a PKA/PLC/PKC/MEK/ERK-dependent pathway: incidence on peroxisome. Mitochondria, and Lipid Profiles, Molecules 24, 3310. https://doi.org/10.3390/molecules24183310.

Nury, T., Zarrouk, A., Vejux, A., Doria, M., Riedinger, J.M., Delage-Mourroux, R., Lizard, G., 2014. Induction of oxiapoptophagy, a mixed mode of cell death associated with oxidative stress, apoptosis and autophagy, on 7-ketocholesterol-treated 158N murine oligodendrocytes: impairment by α-tocopherol. Biochem Biophys Res Commun 446, 714–719. https://doi.org/10.1016/j.bbrc.2013.11.081.

Nury, T., Zarrouk, A., Mackrill, J.J., Samadi, M., Durand, P., Riedinger, J.-M., Doria, M., Vejux, A., Limagne, E., Delmas, D., Prost, M., Moreau, T., Hammami, M., Delage-Mourroux, R., O'Brien, N.M., Lizard, G., 2015. Induction of oxiapoptophagy on 158N murine oligodendrocytes treated by 7-ketocholesterol-, 7β-hydroxycholesterol-, or 24(S)-hydroxycholesterol: protective effects of α-tocopherol and docosahexaenoic acid (DHA; C22:6 n-3). Steroids 99, 194–203. https://doi.org/10.1016/j.steroids.2015.02.003.

Nury, T., Zarrouk, A., Ragot, K., Debbabi, M., Riedinger, J.-M., Vejux, A., Aubourg, P., Lizard, G., 2017. 7-ketocholesterol is increased in the plasma of X-ALD patients and induces peroxisomal modifications in microglial cells: potential roles of 7-ketocholesterol in the pathophysiology of X-ALD. J. Steroid Biochem. Mol. Biol. 169, 123–136. https://doi.org/10.1016/j.jsbmb.2016.03.037.

Nury, T., Sghaier, R., Zarrouk, A., Ménétrier, F., Uzun, T., Leoni, V., Caccia, C., Meddeb, W., Namsi, A., Sassi, K., Mihoubi, W., Riedinger, J.-M., Cherkaoui-Malki, M., Moreau, T., Vejux, A., Lizard, G., 2018. Induction of peroxisomal changes in oligodendrocytes treated with 7-ketocholesterol: attenuation by α-tocopherol. Biochimie 153, 181–202. https://doi.org/10.1016/j.biochi.2018.07.009.

Nury, T., Zarrouk, A., Yammine, A., Mackrill, J.J., Vejux, A., Lizard, G., 2020. Oxiapoptophagy: a type of cell death induced by some oxysterols. Br J Pharmacol. https://doi.org/10.1111/bph.15173.

Nury, T., Yammine, A., Ghzaiel, I., Sassi, K., Zarrouk, A., Brahmi, F., Samadi, M., Rup-Jacques, S., Vervandier-Fasseur, D., Pais de Barros, J.P., Bergas, V., Ghosh, S., Majeed, M., Pande, A., Atanasov, A., Hammami, S., Hammami, M., Mackrill, J., Nasser, B., Andreoletti, P., Cherkaoui-Malki, M., Vejux, A., Lizard, G., 2021. Attenuation of 7-ketocholesterol- and 7β-hydroxycholesterol-induced oxiapoptophagy by nutrients, synthetic molecules and oils: potential for the prevention of age-related diseases. Ageing Res Rev 68, 101324. https://doi.org/10.1016/j.arr.2021.101324.

Oconnor, M.S., Clemens, D., 2022. Cyclodextrin dimers for the remediation of atherosclerotic plaque. Atherosclerosis 355, 94. https://doi.org/10.1016/j.atherosclerosis.2022.06.511.

Pariente, A., Peláez, R., Pérez-Sala, Á., Larráyoz, I.M., 2019. Inflammatory and cell death mechanisms induced by 7-ketocholesterol in the retina. Implications for Age-Related Macular Degeneration, Exp Eye Res 187, 107746. https://doi.org/10.1016/j.exer.2019.107746.

Poli, G., Biasi, F., Leonarduzzi, G., 2013. Oxysterols in the pathogenesis of major chronic diseases. Redox Biol 1, 125–130. https://doi.org/10.1016/j.redox.2012.12.001.

Prieto Tenreiro, A., Penacho Lázaro, M.Á., Andrés Celda, R., Fernández Fernández, M., González Mateo, C., Díez Hernández, A., 2013. Dietary treatment for X-linked adrenoleukodystrophy: is "Lorenzo's oil" useful? Endocrinol Nutr 60, 37–39. https://doi.org/10.1016/j.endonu.2012.01.011.

B. Qiu, M.C. Simon, BODIPY 493/503 Staining of Neutral Lipid Droplets for Microscopy and Quantification by Flow Cytometry, (2016).

Ragot, K., Delmas, D., Athias, A., Nury, T., Baarine, M., Lizard, G., 2011. α-Tocopherol impairs 7-ketocholesterol-induced caspase-3-dependent apoptosis involving GSK-3 activation and Mcl-1 degradation on 158N murine oligodendrocytes. Chem Phys Lipids 164, 469–478. https://doi.org/10.1016/j.chemphyslip.2011.04.014.

Ragot, K., Mackrill, J.J., Zarrouk, A., Nury, T., Aires, V., Jacquin, A., Athias, A., Pais de Barros, J.-P., Véjux, A., Riedinger, J.-M., Delmas, D., Lizard, G., 2013. Absence of correlation between oxysterol accumulation in lipid raft microdomains, calcium increase, and apoptosis induction on 158N murine oligodendrocytes. Biochem Pharmacol 86, 67–79. https://doi.org/10.1016/j.bcp.2013.02.028.

Reichard, J.F., Motz, G.T., Puga, A., 2007. Heme oxygenase-1 induction by NRF2 requires inactivation of the transcriptional repressor BACH1. Nucleic Acids Res 35, 7074–7086. https://doi.org/10.1093/nar/gkm638.

Rezig, L., Ghzaiel, I., Ksila, M., Yammine, A., Nury, T., Zarrouk, A., Samadi, M., Chouaibi, M., Vejux, A., Lizard, G., 2022. Cytoprotective activities of representative nutrients from the Mediterranean diet and of Mediterranean oils against 7-keto-cholesterol- and 7β-hydroxycholesterol-induced cytotoxicity: application to age-related diseases and civilization diseases. Steroids 187, 109093. https://doi.org/10.1016/j.steroids.2022.109093.

Rimbach, G., Minihane, A.M., Majewicz, J., Fischer, A., Pallauf, J., Virgli, F., Weinberg, P.D., 2002. Regulation of cell signalling by vitamin E. Proc Nutr Soc 61, 415–425. https://doi.org/10.1079/pns2002183.

Rodríguez, I.R., Larrayoz, I.M., 2010. Cholesterol oxidation in the retina: implications of 7KCh formation in chronic inflammation and age-related macular degeneration. J Lipid Res 51, 2847–2862. https://doi.org/10.1194/jlr.R004820.

Rothe, G., Valet, G., 1990. Flow cytometric analysis of respiratory burst activity in phagocytes with hydroethidine and 2',7'-dichlorofluorescin. Journal of Leukocyte Biology 47, 440–448.

Royer, M.C., Lemaire-Ewing, S., Desrumaux, C., Monier, S., Barros, J.P., Athias, A., 2009. 7-ketocholesterol incorporation into sphingolipid/cholesterol-enriched (lipid raft) domains is impaired by vitamin E: a specific role for alpha-tocopherol with consequences on cell death. J Biol Chem 284, 15826–15834.

Samadi, A., Sabuncuoglu, S., Samadi, M., Isikhan, S.Y., Chirumbolo, S., Peana, M., Lay, I., Yalcinkaya, A., Bjørklund, G., 2021. A comprehensive review on oxysterols and related diseases. Curr Med Chem 28, 110–136. https://doi.org/10.2174/0929867327666200316142659.

Sassa, T., Wakashima, T., Ohno, Y., Kihara, A., 2014. Lorenzo's oil inhibits ELOVL1 and lowers the level of sphingomyelin with a saturated very long-chain fatty acid. J Lipid Res 55, 524–530.

Sassi, K., Nury, T., Zarrouk, A., Sghaier, R., Khalafi-Nezhad, A., Vejux, A., Samadi, M., Aissa-Fennira, F.B., Lizard, G., 2019. Induction of a non-apoptotic mode of cell death associated with autophagic characteristics with steroidal maleic anhydrides and 7β-hydroxycholesterol on glioma cells. J Steroid Biochem Mol Biol 191, 105371. https://doi.org/10.1016/j.jsbmb.2019.04.020.

Schlegel, R.A., Stevens, M., Lumley-Sapanski, K., Williamson, P., 1993. Altered lipid packing identifies apoptotic thymocytes. Immunology Letters 36, 283–288.

Schloendorn, J., Webb, T., Kemmish, K., Hamalainen, M., Jackemeyer, D., Jiang, L., 2009. Medical bioremediation: a concept moving toward reality. Rejuvenation Res 12, 411–419.

Schwingshackl, L., Morze, J., Hoffmann, G., 2020. Mediterranean diet and health status: active ingredients and pharmacological mechanisms. Br J Pharmacol 177, 1241–1257.

T. Suzuki, J. Takahashi, M. Yamamoto, Molecular Basis of the KEAP1-NRF2 Signaling Pathway, Mol Cells 46 (2023) 133–141. 10.14348/molcells.2023.0028.

Testa, G., Gamba, P., Badilli, U., Gargiulo, S., Maina, M., Guina, T., Calfapietra, S., Biasi, F., Cavalli, R., Poli, G., Leonarduzzi, G., 2014. Loading into nanoparticles improves quercetin's efficacy in preventing neuroinflammation induced by oxysterols. PLoS One 9, e96795.

Testa, G., Rossin, D., Poli, G., Biasi, F., Leonarduzzi, G., 2018. Implication of oxysterols in chronic inflammatory human diseases. Biochimie 153, 220–231.

Vejux, A., Kahn, E., Dumas, D., Bessède, G., Ménétrier, F., Athias, A., Riedinger, J.-M., Frouin, F., Stoltz, J.-F., Ogier-Denis, E., Todd-Pokropek, A., Lizard, G., 2005. 7-ketocholesterol favors lipid accumulation and colocalizes with Nile red positive cytoplasmic structures formed during 7-ketocholesterol-induced apoptosis: analysis by flow cytometry, FRET biphoton spectral imaging microscopy, and subcellular fractionation. Cytometry A 64, 87–100. https://doi.org/10.1002/cyto.a.20124.

Vejux, A., Kahn, E., Ménétrier, F., Montange, T., Lherminier, J., Riedinger, J.M., 2007. Cytotoxic oxysterols induce caspase-independent myelin figure formation and caspase-dependent polar lipid accumulation. Histochem Cell Biol 127, 609–624.

Vejux, A., Guyot, S., Montange, T., Riedinger, J.-M., Kahn, E., Lizard, G., 2009. Phospholipidosis and down-regulation of the PI3-K/PDK-1/Akt signalling pathway are vitamin E inhibitable events associated with 7-ketocholesterol-induced apoptosis. J Nutr Biochem 20, 45–61. https://doi.org/10.1016/j.jnutbio.2007.12.001.

Vejux, A., Abed-Vieillard, D., Hajji, K., Zarrouk, A., Mackrill, J.J., Ghosh, S., Nury, T., Yammine, A., Zaibi, M., Mihoubi, W., Bouchab, H., Nasser, B., Grosjean, Y., Lizard, G., 2020. 7-ketocholesterol and 7β-hydroxycholesterol: in vitro and animal models used to characterize their activities and to identify molecules preventing their toxicity. Biochem Pharmacol 173, 113648. https://doi.org/10.1016/j.bcp.2019.113648.

Vigne, S., Pot, C., 2024. Implication of oxysterols and phytosterols in aging and human diseases. Adv Exp Med Biol 1440, 231–260. https://doi.org/10.1007/978-3-031-43883-7_12.

Walther, T.C., Farese Jr, R.V., 2012. Lipid droplets and cellular lipid metabolism. Annual Review of Biochemistry 81, 687–714.

Wanders, R.J., Waterham, H.R., 2006. Biochemistry of mammalian peroxisomes revisited. Annual Review of Biochemistry 75, 295–332.

Yammine, A., Nury, T., Vejux, A., Latruffe, N., Vervandier-Fasseur, D., Samadi, M., Greige-Gerges, H., Auezova, L., Lizard, G., 2020. Prevention of 7-ketocholesterol-induced overproduction of reactive oxygen species, mitochondrial dysfunction and cell death with major nutrients (polyphenols, ω3 and ω9 unsaturated fatty acids) of the Mediterranean diet on N2a neuronal cells. Molecules 25. https://doi.org/10.3390/molecules25102296.

Yammine, A., Nury, T., Vejux, A., Latruffe, N., Vervandier-Fasseur, D., Samadi, M., Greige-Gerges, H., Auezova, L., Lizard, G., 2020. Prevention of 7-ketocholesterol-induced overproduction of reactive oxygen species, mitochondrial dysfunction and cell death with major nutrients (polyphenols, ω3 and ω9 unsaturated fatty acids) of the Mediterranean diet on N2a neuronal cells. Molecules 25, E2296. https://doi.org/10.3390/molecules25102296.

Yammine, A., Zarrouk, A., Nury, T., Vejux, A., Latruffe, N., Vervandier-Fasseur, D., Samadi, M., Mackrill, J.J., Greige-Gerges, H., Auezova, L., Lizard, G., 2020. Prevention by dietary polyphenols (resveratrol, quercetin, apigenin) against 7-ketocholesterol-induced oxiapoptophagy in neuronal N2a cells: potential interest for the treatment of neurodegenerative and age-related diseases. Cells 9, E2346. https://doi.org/10.3390/cells9112346.

Yammine, A., Ghzaiel, I., Pires, V., Zarrouk, A., Kharoubi, O., Greige-Gerges, H., Auezova, L., Lizard, G., Vejux, A., 2024. Cytoprotective effects of α-linolenic acid, eicosapentaenoic acid, docosahexaenoic acid, oleic acid and α-tocopherol on 7-ketocholesterol – induced oxiapoptophagy: major roles of PI3-K/PDK-1/akt signaling pathway and glutathione peroxidase activity in cell rescue, current research. Toxicology, 100153. https://doi.org/10.1016/j.crtox.2024.100153.

Zarrouk, A., Vejux, A., Mackrill, J., O'Callaghan, Y., Hammami, M., O'Brien, N., Lizard, G., 2014. Involvement of oxysterols in age-related diseases and ageing processes. Ageing Res Rev 18, 148–162. https://doi.org/10.1016/j.arr.2014.09.006.

Zarrouk, A., Nury, T., Karym, E.-M., Vejux, A., Sghaier, R., Gondcaille, C., Andreoletti, P., Trompier, D., Savary, S., Cherkaoui-Malki, M., Debbabi, M., Fromont, A., Riedinger, J.-M., Moreau, T., Lizard, G., 2017. Attenuation of 7-ketocholesterol-induced overproduction of reactive oxygen species, apoptosis, and autophagy by dimethyl fumarate on 158N murine oligodendrocytes. J. Steroid Biochem. Mol. Biol. 169, 29–38. https://doi.org/10.1016/j.jsbmb.2016.02.024.

Zarrouk, A., Martine, L., Grégoire, S., Nury, T., Meddeb, W., Camus, E., Badreddine, A., Durand, P., Namsi, A., Yammine, A., Nasser, B., Mejri, M., Bretillon, L., Mackrill, J.J., Cherkaoui-Malki, M., Hammami, M., Lizard, G., 2019. Profile of fatty acids, tocopherols, phytosterols and polyphenols in Mediterranean oils (argan oils, olive oils, Milk thistle seed oils and nigella seed oil) and evaluation of their antioxidant and cytoprotective activities. Curr Pharm Des 25, 1791–1805. https://doi.org/10.2174/1381612825666190705192902.

Zhang, X., Sivaprasad, S., 2021. Drusen and pachydrusen: the definition, pathogenesis, and clinical significance. Eye (lond) 35, 121–133. https://doi.org/10.1038/s41433-020-01265-4.